ISSN 0018-151X, High Temperature, 2017, Vol. 55, No. 3, pp. 434–456. © Pleiades Publishing, Ltd., 2017.
Original Russian Text © V.I. Khvesyuk, A.S. Skryabin, 2017, published in Teplofizika Vysokikh Temperatur, 2017, Vol. 55, No. 3, pp. 447–471.

REVIEW

Heat Conduction in Nanostructures

V. I. Khvesyuk and A. S. Skryabin*

Bauman Moscow State Technical University, Moscow, 107005 Russia

**e-mail: terra107@yandex.ru*

Received December 4, 2015

Abstract—Specific features of the heat transfer in nanostructures and methods of their investigation are discussed. Phonon heat conduction that is characteristic of semiconductors and insulators is considered. In nanostructures, the Fourier law is violated and the methods of classical theory of heat conduction are inapplicable. Analysis of the physics of heat-transfer processes has shown that the heat conduction of nanostructures depends on the shape and size of the sample, properties of its surface, and direction of the heat flow with respect to the nanostructure geometry. This fact has led to the development of radically new approaches to the determination of thermal conductivity of solids on the nano- and micrometer scales. Therefore, main attention is paid to the review of existing methods for finding thermal conductivity of nanostructures and the results of its theoretical and experimental determination. Various models of heat transfer in nanostructures are presented. The knowledge of statistical thermodynamics, kinetic theory, and solid-state physics is fundamental for this field of thermal physics.

DOI: 10.1134/S0018151X17030129

CONTENTS

INTRODUCTION

For about 25 years, much interest has been shown in thermophysical properties of nano- and microstructures because they are exceptionally promising for almost all fields of science, technology, medicine, etc. Investigations revealed significant differences in the characters of heat transfer in macroscopic solids and small solids with a size from several nanometers to 10–20 μm. Another specific feature of this problem is a great variety of objects, which calls for the development of special theoretical and experimental methods of study. In this context, heat transfer in small solid-state samples is currently an urgent problem [1–8]. A separate line of research is focused on solid-state structures, in which transfer heat is performed via phonons (e.g., graphene, semiconductor materials (including carbon nanotubes), and insulators). This review is devoted to objects in which heat transfer is performed mainly via phonons. We consider the methods of theoretical determination of the thermal conductivity of nanostructures and some calculation results and compare the calculation results with the experimental data.

The l_∞/L ratio determines the character of transfer heat in small solids. This ratio is often referred to as the Knudsen number by analogy with the corresponding dimensionless criterion in gas dynamics. Here, l_∞ is the phonon mean free path in a macroscopic sample, the size of which L is much larger than l_∞. When the case in point is nanostructures, the corresponding characteristic sizes are considered as L. For example, this can be either length or diameter for nanotube, diameter for nanowire, and thickness for film. When the inequality $l_\infty/L < 10^{-3}$ is satisfied for all three dimensions (for macroscopic solids), the classical diffusive heat transfer is implemented, the mechanism of which is determined by the Fourier law $\mathbf{q} = -\kappa_\infty \nabla T$ (T is temperature, $\mathbf{q}$ is the heat flow, and κ_∞ is the thermal conductivity of a macroscopic solid). Another limiting value of the l_∞/L ratio is on the order of 10^2 and corresponds to the so-called Casimir limit $l_\infty/L \gg 1$, when almost all phonons transfer heat between the boundaries of solids without collisions in a solid. This mechanism of heat transfer is referred to as ballistic. Between the above limiting cases (for l_∞/L varying approximately from 10^{-2} to 10; the latter value was obtained in the calculations [9]), the diffusive–ballistic regime is implemented. In this range of variation in l_∞/L, a phenomenon, unknown within the classical theory, occurs: dependence of the thermal conductivity on the sample size. Due to this, the so-called effec-

tive thermal conductivity $\kappa_{eff}(L)$ is introduced. This phenomenon cannot be explained within the phenomenological diffusion-transfer theory based on the Fourier law. The statistical theory of heat conduction of solids is required in this case, which is primarily based on the works by Peierls and Klemens [10, 11]. In this context, the heat transfer in the range of variation in L where $\kappa_{eff} = f(L)$ is often referred to as nondiffusive. The dependence of the thermal conductivity on the sample size is the most important criterion distinguishing heat transfer in nanostructures from that in macrosolids. Therefore, it is very often mentioned in reviews and original papers. However, thermal conductivity also depends on the sample shape. This is confirmed, for example, by the fact that the phonon mean free path differs by a factor of two for nanofilms and nanowires, which have identical thickness and diameter [12]. Another important feature is the anisotropy of thermal conductivity of nanostructures, which manifests itself even for ideal single-crystal samples. This was demonstrated in computational studies of the thermal conductivity for nanofilms [13] and graphene nanoribbons [14].

In view of the aforesaid, it is reasonable to refine the concepts. The point is that the heat flow within and without the Fourier approximation is formally recorded in the same way: $\mathbf{q} = -\kappa_\infty \nabla T$ and $\mathbf{q} = -\kappa_{eff} \nabla T$. The difference consists in the properties of κ_∞ and κ_{eff}. The κ_∞ value is independent of the size and shape of the macroscopic body and the heat-flow direction if the material of which the body is made is homogeneous. In contrast to κ_∞, the κ_{eff} value determining the nondiffusive heat transfer depends on the size and shape of nano- and microstructures, as well as on the heat-flow direction therein:

$$\kappa_{eff} = f\left(L, d, h, \frac{\mathbf{q}}{|\mathbf{q}|}\right),$$

where d is the diameter of a nanowire or nanotube and h is the thickness of a nanofilm. Nondiffusive heat transfer means that a part of heat is transferred by ballistic phonons, which undergo no collisions while moving from one boundary to the opposite.

Specific properties of heat transfer in nanostructures are determined by two factors. The first one is the shape and sizes of the objects under study. The second factor is the presence of mutual phonon interaction of two types in phonon gas. One type is N-processes, characterized by the fact that the total momentum and energy of quasiparticles participating in them are identical before and after the interaction. Correspondingly, the gas as a whole does not lose energy and pulse as well. The second type is U-processes. As a result of interactions of this type, phonons transfer a part of the momentum to the lattice but their total energy does not change. Solutions of the Boltzmann equation taking into account phonon interactions of both types show that, at low temperatures (or $l_\infty / L > 1$), the nondiffusive regime is implemented due to the dominant role of N-processes. In the region of low temperatures or small longitudinal sizes of the nanofilms and nanowires, hydrodynamic heat transfer is implemented, which is a flow of phonon gas as a whole under the action of pressure gradient. Along with the hydrodynamic model, the methods based on the solution of the Boltzmann equation are used to describe the heat transfer in the longitudinal direction. For the transverse direction, the hydrodynamic model is inapplicable. Kinetic methods based on the solution of the Boltzmann equation are applied to describe heat transfer. In both cases, there is the so-called diffusive–ballistic heat transfer, when one part of phonons undergoes interactions in the space between the structure boundaries (diffusive transport), while the other part transfers heat from one boundary to the other without interactions inside the solid (ballistic transport).

Below, we will present theoretical and experimental studies on the aforementioned phenomena, including most recent publications.

The exceptional importance of these studies is related to the development of nanotechnologies, which are very promising for designing radically new systems in the fields of science and technology such as medicine, electronics, optoelectronics, thermoelectric and solar energy converters, materials science, power engineering, etc. All these fields imply the problem of determining thermal conditions that provide stable operation of the designed devices. This problem, in turn, calls for the development of scientific bases of thermal physics of nanostructures (or nano thermal physics), including thermodynamics of nanostructures and theory of heat transfer in them. The studies performed to date show that this division of thermal physics differs significantly (in some concepts) from the classical macroscopic thermal physics and requires the development of radically new theoretical and experimental methods.

It was Fourier who started rigorous investigation of heat transfer processes in solids in his famous work "Analytical Theory of Heat" in 1822, where the Fourier law was formulated. This study gave a start to the development of the classical theory of heat conduction, where heat transfer is considered as a diffusive process. The classical theory of heat conduction is phenomenological and does not specify what objects are heat carriers.

In the early 20th century, two works were presented, which became a basis for the development of statistical solid-state thermodynamics: Einstein's study in 1907 and Debye's study in 1912, which developed significantly the concepts given in the former work. According to Debye, the internal-energy carriers in a solid are classical elastic waves propagating therein. Proceeding from this theory, in 1945, V.V. Tarasov [15, 16] extended for the first time the concepts of solid-state

thermodynamics to two-dimensional and one-dimensional structures which are directly related to nanotechnologies (two-dimensional structures are graphene, silicene, and some others, while nanowires belong to one-dimensional structures).

Development of quantum mechanics led in 1929 to the study by Peierls [10], where the foundations of microscopic theory of heat transfer in solids were laid. The initial concept is quantization of classical elastic waves propagating in a solid. As a result, microscopic analysis of heat transfer is reduced to investigation of the kinetics of gas consisting of quasiparticles (phonons). One of the remarkable properties of this gas is weak mutual interaction of phonons (ideal gas). Therefore, the solution of the Boltzmann equation is sufficient for determining thermal conductivities of various materials, which is widely applied in practice when analyzing properties of rarefied gases and plasma. The corresponding methods for macroscopic solids were developed by Clemens [11].

Up to the early 1960s, studies on the heat transport theory were focused on developing methods for determining thermal conductivity of macroscopic solids. These methods include consideration of phonon scattering both from each other and at various irregularities of the ideal structure of solid-state lattices (e.g., due to the presence of impurities, defects, etc).

In [17], the kinetic equation was solved taking into account only *N*-processes of phonon interaction. It was shown that in this case phonon gas propagates as a whole along nanowires and nanofilms; i.e., the so-called hydrodynamic regime of heat transfer is implemented. Similar investigation was carried out in [18], where *U*-processes and processes of phonon deceleration caused by crystal imperfections were taken into account along with *N*-processes. It was shown that, under the conditions where *N*-processes dominate in phonon gas, the directed momentum acquired by phonon gas under the action of temperature gradient is slowed down only slightly by rare *U*-processes. As a result, a heat-transferring phonon flux occurs. As an example, heat transfer along a rod with a small diameter d was considered in [19]. If the mean free path with respect to *N*-processes l_N is much smaller than the rod diameter $l_N \ll d$ and the mean free path with respect to all possible processes of phonon deceleration is $l_R \gg d$, the regime of continuous phonon flow along the rod is implemented. This situation resembles the Poiseuille gas flow in a tube.

An important property of nondiffusive heat transfer (dependence of κ_{eff} on the sample size) was found for the first time in [19] based on qualitative estimations. A simple qualitative estimation showed that this dependence is power-law:

$$\kappa_{\text{eff}} = AL^{\beta}(\beta > 0), \qquad (1)$$

where L is the sample size. This result was experimentally confirmed for the first time in [20]. Currently, this specific feature is confirmed in many theoretical, numerical, and experimental studies. Modern data yield that the β value is not constant but depends on L (i.e., dependence (1) has a more complex behavior in comparison with the power-law function).

The next two studies are devoted to a more detailed solution of the Boltzmann equation for phonon gas in an ideal crystal in two limiting cases where *N*- or *U*-processes dominate [21, 22]. It was shown that a combined (diffusive and hydrodynamic) regime of heat transfer is implemented in the first case, whereas a purely diffusive regime is implemented in the second case. A system of equations that includes the equations of conservation of energy and momentum of the system (Guyer–Krumhansl (GK) system of equations) was obtained for the hydrodynamic regime. An example of the solution of the GK system of equations was presented in [23]. Note that the solution is reduced to the determination of the effective thermal conductivity.

Finally, we should say that quite complete presentation of the solutions of the Boltzmann equation for phonon gas as applied to different regimes of heat transfer was given in [24]. The results this study are of particular interest because its initial parameters are phonon-gas parameters that differ from those in [21, 22]. The unknown values in [21, 22] are internal energy of phonon gas E and heat flow $\mathbf{q}$ propagating through the material, whereas in [24] the corresponding parameters are temperature T and phonon flux rate $\mathbf{V}$. This is more conventional when analyzing gas flow. We will show below that the systems of equations [21, 22] and [24] are equivalent.

A series of studies have recently been published where the thermal-mass model is developed, which has some common features with the hydrodynamic model but at the same time differs from it. This model is based on the system of hydrodynamics equations [25]. Both models are aimed at analyzing longitudinal heat propagation and are in agreement with the known experimental data.

The kinetic model may compete well enough with the hydrodynamic model [26–29]. It is a modified version of the solution of the Boltzmann equation for macroscopic objects [11]. The difference from the classical formula for thermal conductivity is that the former takes into account the shape and sizes of the object under study and, correspondingly, scattering at boundaries and other possible types of scattering. The classical model is based on the fact that the medium is isotropic (i.e., the phonon mean free paths are identical in all directions). The kinetic model for nanostructures takes into account their real sizes; therefore, the mean free paths differ for different directions.

The kinetic model of heat transfer across a thin film was proposed for the first time in [30]. The Boltz-

mann equation simultaneously taking into account the diffusive and ballistic heat transports is used therein.

Experimental and numerical investigations mainly confirm the theoretical predictions. Dependence of the effective thermal conductivity κ_{eff} on l_∞/L and κ_∞ has approximately the following form: $\kappa_{eff} = \kappa_\infty [L/(L + l_\infty)]$ [31]. Results of these investigations are generally presented in the form of power-law dependences of the thermal conductivity κ_{eff} on the sizes L of nano- and microstructures in separate ranges of sample lengths (1). However, in the entire range (from an infinitely small value to the size where the diffusive mechanism of heat transfer corresponding to macroscopic samples ($\beta = 0$) is established), dependence (1) is a curve, the exponent of power β of which changes with size and, finally, tends to zero. Such dependences were obtained experimentally and numerically [9, 32–36].

Thus, when the sample size gradually increases from a value that is much smaller than the phonon mean free path (when the nondiffusive regime of heat conduction is dominant) to sizes significantly exceeding the mean free path (when the classical diffusive mechanism of heat transfer is established), the effective thermal conductivity of the sample increases up to the κ_∞ values that are typical of large three-dimensional samples. During the increase in the size, the heat transfer is simultaneously provided by the aforementioned mechanisms: diffusive and ballistic. Contribution to the heat transfer from each mechanism changes with an increase in the sample size until only one (diffusive) mechanism remains.

We should note that there is a great variety of nanostructures, analysis of the heat-transfer processes in which may differ significantly from the above-considered examples. These structures include superlattices and some other types of multilayer structures. In addition, specific approaches are used for studying heat transfer in the objects such as graphene, graphane, and silicene, as well as closely related nanoribbons, layer graphene, graphite, etc. Therefore, one should take into account that the focus of this review is primarily on the objects such as thin films, nanowires, and nanotubes.

PRINCIPLES OF MICROSCOPIC HEAT TRANSFER IN SOLIDS

In this section, we present information that is necessary for detailed analysis of the heat-transfer processes in nanostructures. Here, we discuss two fundamental problems: first, microscopic specific features of the phonon interaction (or mutual transformation) processes because these processes lead to the elimination of one particles and occurrence of the others (as for any quasiparticles); second, physical pattern of two mechanisms of heat transport via phonons, which proceeds from physics of phonon creation and annihilation processes.

The Fourier law introduces the concept of thermal conductivity. However, this parameter became possible to calculate only after 1929, when Peierls introduced the concept of phonons: quanta of waves propagating in solids. The existence of quasiparticles (phonons) became the basis for the microscopic theory of heat conduction in insulators and semiconductors.

Phonons are space-limited wave excitations of a solid lattice (wave packets). Their state is characterized by frequency ω, energy $\hbar\omega$, and quasi-momentum $\mathbf{p} = \hbar\mathbf{k}$. Parameter $\mathbf{k}$ is the wave vector with magnitude at $2\pi/\lambda$, where λ is the wavelength. The role of quasi-momentum in the theory is similar to that of the conventional momentum in continuous free space. The difference between them is caused by the fact that quasi-momentum propagating in discrete space formed by the solid lattice is determined accurate to vector $\hbar\mathbf{b}$, where $\mathbf{b}$ is the reciprocal lattice vector. Phonons, the momenta of which differ by $\hbar\mathbf{b}$, have identical energy. A periodic lattice containing N sites corresponds to $N - 1$ nonzero values of vector $\mathbf{b}$.

Specific features of phonon interactions with each other and with the solid lattice play a key role in the further presentation. Microscopic properties of quasiparticles determine macroscopic properties of the phonon gas as a whole. This gas exists inside the solid lattice. This is the first reason for the significant difference in the behaviors of conventional gases composed of atoms and molecules existing in continuous medium from phonon gas existing in a discrete medium. The second reason is that atoms and molecules are real particles with real mass, whereas phonons are vibrational excitations of the solid lattice with zero mass.

To establish the most important properties of crystalline solids, one should find the dependences of frequencies ω of the waves propagating in a solid on wave vectors $\omega(\mathbf{k})$. These functions are referred to as dispersion relations. They are determined within the classical theory of elastic harmonic waves [37] and remain valid for phonons.

Here, we restrict ourselves to the consideration of the results of solving the problem of vibrations of a one-dimensional chain of identical atoms, the equilibrium positions of which are spaced by identical mean distances a. The specific feature of crystalline solids is that the wavelengths of waves propagating in them cannot be smaller than the lattice constant a: $\lambda = \lambda_{min} > a$. This value corresponds to the phonon wave vector $\mathbf{k}_m$. The magnitude of the wave vector changes from 0 to $\mathbf{k}_m$. The complete solution to the classical problem of propagation of vibrations in a one-dimensional lattice of atoms of identical mass, the repulsive forces between which are proportional to the distances between them, was obtained by Kelvin in 1881 [16]. The dispersion equation has the form

$$\omega(k) = \left(\frac{4\alpha}{M}\right)^{1/2}\left|\sin\left(\frac{ka}{2}\right)\right|,$$

where α is the constant representing the interaction forces between neighboring atoms and M is the mass of lattice atoms. It follows from this formula that the maximum possible wave-frequency value is $\omega_{max} = (4\alpha/M)^{1/2}$.

It follows from the above formula that one $\omega(k)$ value corresponds to many k values. There is some range of allowable k values from 0 to k_m in the one-dimensional k-space, which is characterized by one-to-one correspondence between ω and k. As follows from the dispersion relation, in this case this range is $-\pi/a \le k \le \pi/a$. It is referred to as the first Brillouin zone. When considering two- or three-dimensional lattices, the Brillouin zones have the corresponding dimensions. Point $\mathbf{k} = 0$, equal to infinite wavelength, is generally at the zone center. The region in the vicinity of point $|\mathbf{k}| \ll 1/a$ corresponds to low-frequency long-wavelength phonons, while the region near $|\mathbf{k}| \sim 1/a$ corresponds to short-wavelength phonons. Beyond the first zone of k-space, there are other zones of positive and negative k values, magnitudes of which exceed k_m.

An important fundamental property of phonon gas is that the k values are formally limited by nothing, whereas dependences $\omega(\mathbf{k})$ plotted above the k axis periodically take a value from zero to ω_{max}.

Let us now consider the dynamics of phonon interaction. In the general case, the mean free path of phonons is determined by their mutual interactions, presence of various defects in the lattice (impurities, dislocations, etc.), and finite crystal sizes (interaction with boundaries). Here, we consider only the first effect inherent in ideal crystals.

Within this approximation, the problem is reduced to analysis of phonon interactions. In an overwhelming majority of cases, the theory takes into account only the processes which involve three phonons, because the higher-order processes are vanishingly weak. There are two possibilities for such transformations. The first one is decay of one phonon into two phonons. The second possibility is fusion of two phonons with the formation of one phonon. These processes change the total number of particles in the system. The equilibrium energy distribution (Bose–Einstein distribution) is valid for phonons as particles with zero spin:

$$N_0(\omega) = \left(\exp\left(\frac{\hbar\omega}{k_B T}\right) - 1\right)^{-1}. \quad (2)$$

Analysis of the aforementioned processes of interaction (transformation) of particles is carried out using equations representing the energy and quasi-momentum conservation laws.

The quasi-momentum conservation law can be recorded in two ways, depending on the type of processes. One type implies normal processes (N-processes). In this case, all three quasi-momenta belong to the first Brillouin zone. The most important property of these processes is equality of the quasi-momenta before and after the interaction:

$$\mathbf{k}_1 + \mathbf{k}_2 = \mathbf{k}_3,$$

$$\mathbf{k}_1 = \mathbf{k}_2 + \mathbf{k}_3.$$

Note that Planck's constant is omitted in these formulas.

Processes of the second type are referred to as Umklapp-processes (U-processes). These processes occur when particles, for which $|\mathbf{k}| > k_m$, participate in the interaction. The momentum of particles with such $|\mathbf{k}|$ value is determined accurate to $\hbar\mathbf{b}$. The quasi-momentum conservation equation is written so that the values of quasi-momenta, arising after events of particle fusion or decay, are in the first Brillouin zone. This can be achieved by introducing vector $\mathbf{b}$ into the corresponding equations:

$$\mathbf{k}_1 + \mathbf{k}_2 = \mathbf{k}_3 + \mathbf{b}, \quad (3)$$

$$\mathbf{k}_1 = \mathbf{k}_2 + \mathbf{k}_3 + \mathbf{b}. \quad (4)$$

The $\mathbf{b}$ value is determined as follows. Let $\mathbf{a}_1$, $\mathbf{a}_2$, and $\mathbf{a}_3$ be the main lattice periods. Vector $\mathbf{b}$ should satisfy the conditions [36]

$$\mathbf{a}_1 \cdot \mathbf{b} = 2\pi p_1, \quad \mathbf{a}_2 \cdot \mathbf{b} = 2\pi p_2, \quad \mathbf{a}_3 \cdot \mathbf{b} = 2\pi p_3,$$

where p_1, p_2, and p_3 are positive or negative integers. Solution of the written equations yields

$$\mathbf{b} = p_1\mathbf{b}_1 + p_2\mathbf{b}_2 + p_3\mathbf{b}_3.$$

Here, vectors $\mathbf{b}_i$ are determined by the relations

$$\mathbf{b}_1 = \frac{2\pi}{v}[\mathbf{a}_2\mathbf{a}_3], \quad \mathbf{b}_2 = \frac{2\pi}{v}[\mathbf{a}_3\mathbf{a}_1], \quad \mathbf{b}_1 = \frac{2\pi}{v}[\mathbf{a}_1\mathbf{a}_2],$$

$$v = \mathbf{a}_1[\mathbf{a}_2\mathbf{a}_3].$$

Equations (3) and (4) indicate the following. Let the total vector $\mathbf{k}_1 + \mathbf{k}_2$ be beyond the first Brillouin zone and vector $\mathbf{k}_3$, determined from the relation $\mathbf{k}_1 + \mathbf{k}_2 = \mathbf{k}_3 + \mathbf{b}$, be in it. Vector $\mathbf{b}$ provides the presence of vector $\mathbf{k}_3$ in the first Brillouin zone. As a result of this interaction, momentum $\mathbf{b}$ is transferred from phonon gas to the lattice. Due to the periodicity of the lattice and specially chosen reciprocal lattice vector $\mathbf{b}$, the condition $(\mathbf{k}_3) = (\mathbf{k}_3 + \mathbf{b})$ is satisfied. Since the frequency remains constant, the energy is conserved. Accordingly, the energy conservation law has two evident forms:

$$\omega(\mathbf{k}_1) + \omega(\mathbf{k}_2) = \omega(\mathbf{k}_3),$$

$$\omega(\mathbf{k}_1) = \omega(\mathbf{k}_2) + \omega(\mathbf{k}_3).$$

Note that, among three phonons, either all three or only one can be low-energy and long-wavelength [24]. In the case of two long-wavelength and one short-wavelength phonons, the energy and quasi-momentum conservation laws cannot be satisfied.

Physically, the difference between N- and U-processes is as follows. In the case of N-processes, the phonon-gas energy and momentum are conserved. In the case of U-processes, the momentum is transferred from phonon gas to lattice with the total energy conserved.

Thus, according to modern concepts, heat transfer in solids (insulators and semiconductors) is performed via phonon gas. Phonons weakly interact with each other. This is due to the fact that the vibration amplitude of particles of a solid is small in comparison with mean distances between them; therefore, the properties of phonon gas can be investigated using the solutions to the kinetic equation. This equation differs from the Boltzmann equation because the classical collision operator of this equation is inapplicable to phonons. The so-called transport Boltzmann equation is used [10, 11, 17, 19, 21, 22] (see below).

Now let us consider the physical pattern of heat transport by phonons, which is closely related to the specific features of phonon interaction with each other and with the lattice inside the solid. The consideration is performed for ideal crystals; therefore, only the gas retardation due to U-processes is taken into account.

The heat transfer occurs in the presence of temperature gradient and, correspondingly, pressure gradient in phonon gas. This gradient influences phonon gas, which may lead to its motion as a whole. However, under the conventional conditions (room temperature or higher, macroscopic sizes of solids), the relations $l_U/l_N \cong \nu_N/\nu_U \ll 1$ for the phonon mean free paths with respect to normal processes (l_N) and U-processes (l_U) and the corresponding interaction rates (ν_N and ν_U) are satisfied. Under these conditions, the retardation due to U-processes provides immobility of phonon gas. In this case, heat transfer is caused by mutual collisions of phonons from regions with different temperatures (i.e., by diffusive processes).

The situation is quite different when the inverse relations are satisfied (i.e., the retardation due to U-processes is insufficient to provide the gas immobility). In such cases, heat transfer is caused by the motion of phonon gas as a whole. This mechanism is implemented when N-processes dominate.

It should be noted that, under real conditions, some other factors decelerating gas motion occur along with U-processes (for example, lattice defects, impurity atoms, polycrystalline structure, etc.). These factors produce approximately constant retardation in the entire volume of the solid; thus, if gas moves, its velocity is constant across the flow. The mean free path characterizing retardation of the flow under these conditions is l_R. It takes into account all factors in the solid volume that decelerate gas motion due to the action of temperature gradient. Another factor retarding gas motion is phonon scattering from the boundaries of a small solid. An example is heat transfer along nanowires with diameter d. In such cases, $l_R \sim d$, and phonon-gas flows similar to Poiseuille flows of conventional gases in tubes arise, provided that the momentum loss due to the retardation at boundaries dominate.

DIFFUSIVE HEAT TRANSFER

It follows from the Fourier law that the problem of heat transfer in the diffusive regime is reduced to the determination of phonon-gas thermal conductivity κ. Analysis of the transport processes in phonon gas is performed in a similar way as for conventional gases: based on the kinetic equation [10, 11]. The diffusive regime is implemented in macroscopic solids at rather high temperatures. The further presentation concerns heat transport in bulk three-dimensional solids.

The Boltzmann equation is written for the non-equilibrium distribution function $N = N_g(t, \mathbf{r}, \mathbf{k})$, which is determined by solving this equation. Here, t and $\mathbf{r}$ are, respectively, time and space variables and g indicates the wave type. Low-frequency acoustic elastic waves of three types propagate in bulk three-dimensional solids: one longitudinal wave (LA) and two transverse waves (TA) [16]. This circumstance results in low-frequency spectrum of phonon frequencies. High-frequency optical waves also propagate in solids; however, they do not make significant contribution to the thermal conductivity because of low group velocity and, therefore, are generally disregarded. The kinetic equation has the form

$$\frac{\partial N}{\partial t} + \mathbf{u}\frac{\partial N}{\partial \mathbf{r}} = St(N).$$

Here, the wave group velocity $\mathbf{u} = \partial\omega/\partial\mathbf{k}$ determines the phonon velocity and $St(N)$ is the operator of quasiparticle collisions.

Further analysis is carried out within the ideal-crystal approximation where mutual phonon interactions are assumed to be the only type of phonon interactions. The collision integral in the kinetic equation takes into account three-phonon interaction processes. Processes involving four or more phonons are disregarded because their contribution is negligible.

As was noted above, the number of particles in phonon gas is not retained; however, the total energy is conserved within the ideal-crystal approximation. Therefore, using the conventional procedure of reducing the Boltzmann equation to the system of conservation equations (multiplication by particle energy $\hbar\omega$ and integration from 0 to ω_{max}), we obtain for the gas-energy equation (ω and k are related by the dispersion relation $\omega(k)$)

$$\sum_g \int \hbar\omega St(N) \frac{d^3k}{(2\pi)^3} = 0.$$

Here, the summation is over the aforementioned longitudinal and transverse waves (they are also referred to as polarizations). As a result, we have the energy equation in the form

$$\frac{\partial E}{\partial t} + \mathrm{div}\mathbf{q} = 0, \quad (5)$$

where E is the specific internal energy and $\mathbf{q}$ is the heat flow density:

$$E = \sum_g \int \hbar\omega N \frac{d^3k}{(2\pi)^3}, \quad \mathbf{q} = \sum_g \int \hbar\omega \mathbf{u} N \frac{d^3k}{(2\pi)^3}. \quad (6)$$

Let us consider the solution of the equation in the region of relatively high temperatures in macroscopic solids. Under the action of temperature gradient, phonon gas acquires an excess momentum directed opposite to the temperature gradient. However, the rate of U-processes of phonon interaction is high in this temperature region, which leads to the suppression of the directed momentum of phonon gas: it remains immobile. With the other reasons (lattice defects, impurities, etc.) absent, momentum loss in collisions of phonons is the only factor determining the thermal resistance of a solid. Under these conditions, heat transport is determined by the processes of quasiparticle diffusion proceeding from the Fourier law: $\mathbf{q} = -\kappa_\infty \nabla T$. The problem is reduced to derivation of the expression for thermal conductivity. In this case, the simplified expression for the collision operator in the kinetic equation, which is sometimes referred to as τ-approximation, is generally used [11]:

$$St(N) = \frac{N_0 - N}{\tau}.$$

Here, N_0 is equilibrium distribution function (2) and τ is the relaxation time. This time generally depends on ω. However, when solving the kinetic equation, the so-called "gray" approximation, which does not take into account the dependence $\tau(\omega)$ but uses its averaged constant value, is applied in some cases. Within this approximation, taking into account the temperature gradient, this equation has the following form:

$$\frac{\partial N}{\partial t} + (\mathbf{u} \cdot \nabla T)\frac{\partial N}{\partial T} = \frac{N_0 - N}{\tau}.$$

In English-speaking literature, such equations are generally referred to as the Boltzmann transport equations (BTE).

The stationary problem is solved within the linear approximation of small deviations of the distribution function from the equilibrium one. The degree of smallness n of deviations of the distribution function from the equilibrium function is easily written by comparing the function norms: $\|N - N_0\| = \|n\| \ll \|N_0\|$. Specifically parameter n determines the thermal conductivity of phonon gas. Under these conditions, the initial collision integral is transformed into the linearized collision integral $St(N) \to I(n) = -n/\tau$. Further simplification of the Boltzmann equation is reduced to replacement of $\partial N/\partial T$ with $\partial N_0/\partial T$. We have

$$(\mathbf{u} \cdot \nabla T)\frac{\partial N_0}{\partial T} = -\frac{n}{\tau}.$$

Hence,

$$n = -\tau(\mathbf{u} \cdot \nabla T)\frac{\partial N_0}{\partial T}.$$

Here, all parameters (except for temperature) are functions of the wave vector $\mathbf{k}$. Substituting n instead of N into the above expression for heat flow $\mathbf{q}$, we obtain (summation is over the types of waves propagating in the solid)

$$\mathbf{q} = -\sum_g \int \hbar\omega_g \tau_g (\mathbf{u}_g \cdot \nabla T)\mathbf{u}_g \frac{\partial N_0}{\partial T}\frac{d^3k}{(2\pi)^3}.$$

The temperature gradient is taken outside the integral sign. Then the previous expression is reduced to the Fourier law

$$\mathbf{q} = -\kappa_\infty \nabla T,$$

where the thermal conductivity κ_∞ is determined by the formula

$$\kappa_\infty = \frac{1}{3}\sum_g \int \hbar\omega u_g^2 \tau \frac{\partial N_0}{\partial T}\frac{d^3k}{(2\pi)^3} = \frac{1}{3}\sum_g \int Cul\frac{d^3k}{(2\pi)^3}, \quad (7)$$

$C(\omega) = \hbar\omega(dN_0/dT)$ is the specific heat per unit volume, u is the speed of sound, and $l = u\tau$ is the phonon mean free path.

The following formula is often used for simple estimations within the Debye approximation:

$$\kappa_\infty = \frac{1}{3}Cul,$$

where all parameters are averaged over the entire phonon spectrum from zero to ω_{max}.

MODELS OF THE NONDIFFUSIVE REGIME OF HEAT TRANSFER

Before we begin to consider the models that are used for describing the nondiffusive regime of heat transfer in nanostructures, we note one specific feature of the physics of these phenomena: in many cases, the character of heat transport and, correspondingly, the effective thermal conductivity depend on the heat-flow direction. This fact necessitates the development

of models for determining κ_{eff}, which radically differ from each other depending on the heat-flow direction.

Let us clarify the physical meaning of these differences by an example of nanofilm [13]. When heat propagates along the surface of a film with large Knudsen parameter, a phonon-gas flow occurs simultaneously in the same direction [13, 38]. The hydrodynamic component plays an important role in this case. As will be shown below, under these conditions, *N*-processes of phonon interaction generate a part of heat flow in close connection with the processes of scattering at boundaries. The *U*-processes and phonon interactions with lattice defects naturally make a particular contribution.

When heat propagated across the film surface, no gas-dynamic flow is formed, and the problem of heat transport can be solved by only using kinetic methods.

Accordingly, there are two groups of models. The models describing longitudinal transport include hydrodynamic [21–24] and thermal-mass [25] models, as well as kinetic model [26–29] which uses modified expression of classical thermal conductivity (7) and thus takes into account the shape and sizes of the object under study. The models describing transverse transport include diffusive–ballistic [30] and radiative phonon [8] models.

Differences of the mechanisms and, correspondingly, methods of analysis of nondiffusive heat transfer from each other and from the classical diffusion mechanism are discussed below. The models that analyze longitudinal heat transport are first discussed.

As the first example, we consider the so-called hydrodynamic mechanism, found theoretically about 50 years ago [17–22, 24] as a result of accurate solution of the Boltzmann equation (see also [39]), as applied to $\mathrm{Kn} \geq 1$ and low temperatures. The hydrodynamic macroscopic system of equations including the energy and quasi-momentum conservation equations was obtained for phonon gas in [21, 22]. The solution of this system of equations makes it possible to determine the effective thermal conductivities of nano- and microstructures [9, 23]. The kinetic equation is initial for deriving this system of equations. Two factors facilitate the occurrence of the hydrodynamic regime of heat transfer. First, low temperatures (on the order of several kelvin). Second, small sizes of solids (below 10 μm at about 300 K).

It was shown in the previous section that the hydrodynamic regime of heat transport is implemented when the pressure gradient due to temperature inhomogeneity affects phonon gas more strongly as compared with retardation caused by various interactions of quasiparticles with the lattice.

When the case in point is low temperatures, the transition to the hydrodynamic regime is due to the exponential decrease in the rate of *U*-processes with a decrease in temperature to several units of kelvin. Concerning small sizes, the decrease in the rate of processes retarding the gas is due to the increase in the number of ballistic quasiparticles that do not interact with the lattice and to the significant deviation of the distribution function from equilibrium.

The importance of theoretical predictions of the aforementioned studies is that they were confirmed experimentally for both relatively large samples (on the order of several centimeters) at several kelvin [20] and nanostructures at room temperature or higher [40]. Thermal conductivity of small samples does not equal large three-dimensional solids. Therefore, instead of the thermal conductivities of macroscopic samples κ_∞ given in handbooks, the so-called effective thermal conductivities κ_{eff}, which are smaller and depend on sample sizes, are introduced. These dependences have a complex form; however, power-law dependences (1) can be used within relatively small ranges of variation in the sizes.

Let us first consider the physical meaning of the nondiffusive mechanism of heat transfer. As previously, an ideal crystal, which has no impurities, defects, and other factors inducing phonon deceleration, is investigated in the first approximation. When considering longitudinal heat transfer in films and wires, the main factor causing nondiffusive transport is phonon scattering at boundaries. Since the mean free path l_∞ significantly exceeds the film thickness or wire diameter, a part of phonons are ballistic (i.e., they propagate from one boundary to the other without collisions). Diffusion and specular phonon reflections from boundaries are considered. Diffusion phonon scattering at boundaries reduces significantly the effective mean free paths and effective thermal conductivities upon a decrease in nanosizes of the corresponding objects in comparison with macroscopic samples made of the same materials. The resulting heat-transport mechanism is a phonon-gas flow along the nanostructure. In the case of transverse heat transfer, a decrease in the nanosizes also facilitates the increase in the fraction of heat transfer via ballistic mechanism.

We return to specific features of longitudinal heat transport. If the gas-dynamic regime is implemented under the corresponding conditions, there is a phonon-gas flow with the kinematic viscosity at $\mu = l_N \langle u \rangle$ ($\langle u \rangle$ is the mean wave group velocity). This means that a close-to-Poiseuille phonon-gas flow arises in the sample [23, 38]. In such cases, *N*-processes actively participate in the formation of profile of the phonon flow velocity; therefore, they determine an important parameter: mean gas-flow velocity. The mean phonon-flow velocity depends on the phonon-gas viscosity, i.e., on l_N. If the condition $l_N \geq L$ is satisfied, the free-molecular regime of strongly rarefied gas flow is implemented [41]. Concerning the heat-transfer character, we can say that the diffusive–ballistic mode is

implemented. Thus, the heat transport is due to the phonon-gas motion as a whole with some mean velocity **V**.

It follows from the aforesaid that macroscopic energy and quasi-momentum conservation equations, taking into account the specific features of phonon interactions with each other and with the lattice of a solid, should be derived to determine heat transport within the hydrodynamic approximation. This problem can be solved proceeding from the Boltzmann equation. To this end, first, one should accurately write the collision operator in the kinetic equation taking into account *N*- and *U*-processes. Second, one should conventionally reduce the kinetic equation to the system of hydrodynamic equations of energy and quasi-momentum. There are different performance versions of these procedures [21, 22, 24, 39]. Below, we will briefly describe the last version [24].

Derivation of the energy equation from kinetic equation (5), (6) was earlier presented. To obtain the quasi-momentum conservation equation, we should find the solution to the Boltzmann equation that takes into account three-phonon interaction processes. As usual, the linear approximation is used; therefore, the desired distribution function $N(t,\mathbf{r},\mathbf{k})$ is presented in the form of the equilibrium distribution function $N_0(T,\omega)$ plus small correction n taking into account the specific features of this regime. Since the case in point is gas-dynamic flow, the correction takes into account velocity **V** of the phonon flow as a whole. Therefore, argument ω of the distribution function is replaced with $\omega - \mathbf{k}\cdot\mathbf{V}$. At rather small **V** values, the nonequilibrium distribution function can be written as

$$N(\omega - \mathbf{k}\cdot\mathbf{V}) = N_0 - \mathbf{k}\cdot\mathbf{V}\frac{\partial N_0(\omega)}{\partial\omega}. \quad (8)$$

In the general case, it is convenient to introduce desired small corrections χ:

$$n = -\frac{\partial N_0}{\partial\omega}\chi = N_0(N_0+1)\left(\frac{\hbar}{k_B T}\right)\chi.$$

According to (8), $\chi = \mathbf{kV}$.

Then the Boltzmann equation within the stationary approximation has the form

$$\mathbf{u}\cdot\nabla T\frac{\partial N_0}{\partial T} = I_N(\chi) + I_U(\chi), \quad (9)$$

where $\mathbf{u} = \partial\omega/\partial\mathbf{k}$ is the group velocity and $I_N(\chi)$, and $I_U(\chi)$ are the linear operators acting on χ taking into account phonon interaction. Here, the collision integral is divided into parts that separately take into account normal processes (I_N) and umklapp processes (I_U). As usual, each of the operators is a difference between the number of processes per unit time, which lead to the occurrence of phonons in a specified state $(g,\mathbf{k})$, and the number of processes, which bring out phonons from this state. The parameters determining the linear nonequilibrium components of the distribution functions can be written as

$$\chi = \chi_N + \chi_U,$$

where $\chi_N = \mathbf{k}\cdot\mathbf{V}$ and χ_U is the part of the correction to the distribution function that takes into account umklapp processes. Within the approximation under consideration, $\chi_U \ll \chi_N$; accordingly, for the interaction rates, we have $\nu_U \ll \nu_N$. We write

$$I_N(\chi) = I_N(\chi_N + \chi_U) \cong I_N(\chi_N) + I_N(\chi_U) = I_N(\chi_U),$$

because $I_N(\chi_N) = 0$. Similarly,

$$I_U(\chi) = I_U(\chi_N + \chi_U) = I_U(\chi_N) + I_U(\chi_U) = I_U(\chi_N),$$

because $I_U(\chi_U) \ll I_U(\chi_N)$ due to the aforesaid.

As a result, the Boltzmann equation has the form

$$\mathbf{u}\cdot\nabla T\frac{\partial N_0}{\partial T} = I_N(\chi_U) + I_U(\chi_N).$$

Afterward, to obtain the quasi-momentum conservation equation, we multiply all terms of this equation by $\hbar\mathbf{k}$, integrate over $d^3k/(2\pi)^3$, and sum over all polarizations (longitudinal and transverse) of the phonon spectrum. Since normal processes conserve the total quasi-momentum, the integral of $I_N(\chi_U)$ turns to zero. The result of integration is reduced to the quasi-momentum conservation equation

$$\sum_g\int\mathbf{k}(\mathbf{u}\cdot\nabla)T\frac{\partial N_0}{\partial T}\frac{d^3k}{(2\pi)^3} = \sum_g\int\mathbf{k}I_U(\chi_N)\frac{d^3k}{(2\pi)^3}.$$

The left-hand side of this equation determines the process of formation of the phonon-gas flow under the action of temperature gradient and, therefore, pressure gradient; the right-hand side establishes the resistance to its directed motion caused by the presence of *U*-processes. Therefore, the last equation determines the unknown velocity **V**. After substituting $\chi_N = \mathbf{k}\cdot\mathbf{V}$ into the last equation, it takes the form [24]

$$\beta_1\nabla T = -\nu_U\beta_2 T\mathbf{V}, \quad (10)$$

where ν_U is the umklapp collision rate and β_1 and β_2 are determined by the expressions [24]

$$\beta_1 = \frac{1}{3}\frac{\partial}{\partial T}\left(\sum_g\int\mathbf{k}\cdot\mathbf{u}N_0\frac{d^3k}{(2\pi)^3}\right),$$

$$T\nu_U\beta_2 = -\frac{1}{3}\sum_g\int\mathbf{k}I_U(\mathbf{k})\frac{d^3k}{(2\pi)^3}.$$

We find the phonon flow velocity **V** at a specified temperature gradient from Eq. (10). The physical meaning of the term on the right-hand side of the equation is obvious: it means the flow retardation due to the action of only *U*-processes. These processes act with a constant density in the entire volume of the

solid, and the scattering at boundaries is not taken into account here.

Equation (10) is valid for large samples, in which the friction between gas and boundaries is disregarded. However, when the phonon-gas flow in nanowires and nanofilms is under consideration, it is necessary to take into account phonon scattering at surfaces. This scattering leads to the flow retardation by a wall, as a result of which inhomogeneous transverse velocity distribution is formed due to the presence of phonon-gas viscosity which must be taken into account in Eq. (9). This equation for an ideal crystal with the presence of phonon scattering at boundaries can be written as

$$\frac{\beta_1}{\beta_2 T}\nabla T = \mu\Delta\mathbf{V} - \nu_U\mathbf{V}.$$

Here, the temperature gradient is directed along the system axis and the second derivative of velocity takes into account transverse inhomogeneity of the phonon-gas velocity along the tube. The kinematic viscosity of phonons is determined by N-processes [24]: $\mu = l_N\langle u\rangle$. In the case of nonideal crystals, it would be correct to write the last equation in the form

$$\frac{\beta_1}{\beta_2 T}\nabla T = \mu\Delta\mathbf{V} - \nu_R\mathbf{V}, \qquad (11)$$

where ν_R is the rate of phonon collisions related to the loss of quasi-momentum. This parameter takes into account U-processes and events of phonon interaction with irregularities of the lattice geometry. Note that the introduction of viscosity term states a nontrivial problem of formulating the conditions at the boundaries of a solid when solving problems of phonon-gas propagation in solids [23, 39, 42, 43]. Note the difference between Eq. (11) and the motion equation of conventional viscous gas in a tube [44]:

$$\eta\Delta\mathbf{V} = \nabla p$$

(η is the dynamic viscosity). The physical difference is that the last term in (11) takes into account the action of not only surface but also volume retardation on the phonon gas. This term can be neglected when analyzing heat transport, for example, in a nanowire if the condition $\mu/R^2 \gg \nu_U$ is satisfied (R is the nanowire radius).

The expression for the energy flux $\mathbf{q}$ transferred by phonons under the action of temperature gradient is determined in the same way as and in the previous section. Expression (5) is used for $\mathbf{q}$ where the correction to the distribution function n is substituted instead of N; in this case, this correction has the form

$$n = -\mathbf{k}\mathbf{V}\frac{\partial N_0}{\partial\omega} = \mathbf{k}\mathbf{V}\frac{T}{\omega}\frac{\partial N_0}{\partial T}.$$

After substituting this expression into (6), we have $\mathbf{q} = T\beta_1\mathbf{V}$. Then we substitute $\mathbf{V}$ from (10), and the final expression is written as

$$\mathbf{q} = -\kappa_\infty\nabla T,$$

where $\kappa_\infty = \beta_1^2/\nu_U\beta_2$ is the thermal conductivity in infinite medium. This result is obtained for relatively low temperatures. Parameter ν_U exponentially depends on temperature; therefore, κ_∞ is proportional to $\exp(\theta/T)$ [10]. At temperatures above the Debye temperature, the thermal conductivity is inversely proportional to temperature [24].

An interesting result is found if energy equation (5) is written in somewhat different form [24]. We proceed from the expression for N:

$$N = N_0(\omega) - \mathbf{k}\mathbf{V}\frac{\partial N_0}{\partial\omega} = N_0(\omega) + \mathbf{k}\mathbf{V}\frac{T}{\omega}\frac{\partial N_0(\omega)}{\partial T}.$$

We substitute the former expression into formula for E (6) and the latter into the formula for $\mathbf{q}$ from (6). Since the integral of $\hbar\omega\mathbf{k}\mathbf{V}\partial N_0/\partial\omega$ for integration over all directions $\mathbf{k}$ turns to zero, we restrict ourselves to the equilibrium value of the internal energy: $E_0 = \beta_3 T$, where $\beta_3 = \partial E_0/\partial T$. When calculating $\mathbf{q}$, we take into account that the integral of $\omega\mathbf{u}N_0$ also turns to zero and neglect the term containing $\mathbf{V}\nabla T$ [24]. As a result, we obtain $\mathbf{q} = \beta_1 T\mathbf{V}$. Then the energy conservation equation can be written as

$$\beta_3\frac{\partial T}{\partial t} + \beta_1 T\,\mathrm{div}\mathbf{V} = 0. \qquad (12)$$

This implies that $\mathrm{div}\mathbf{V} = 0$ within the stationary approximation; i.e., the phonon gas behaves like incompressible gas.

The quasi-momentum conservation equation within stationary approximation (10) was obtained above. Now let us take into account the nonstationary term of the Boltzmann equation. We have the nonstationary quasi-momentum conservation equation

$$\beta_2 T\frac{\partial\mathbf{V}}{\partial t} + \beta_1\nabla T = +\mu\Delta\mathbf{V} - \nu_R\beta_2 T\mathbf{V}. \qquad (13)$$

Two last equations (12) and (13) have the form found in [24] and are a system of equations for phonon flow taking into account the friction between it and the boundary surfaces. However, one can show that quasi-momentum conservation equation (12) is nonequivalent to the similar equation obtained in [21, 22]: the term having the form of $\nabla(\nabla\mathbf{V})$ is not in (12). The corresponding term taking into account gas compressibility can be taken from the Navier–Stokes equation [44]. Then, the quasi-momentum conservation equation has the form

$$\beta_2 T\frac{\partial\mathbf{V}}{\partial t} + \beta_1\nabla T = \mu\left(\Delta\mathbf{V} + \frac{1}{3}\nabla(\nabla\cdot\mathbf{V})\right) - \nu_R\beta_2 T\mathbf{V}. \qquad (14)$$

The introduced terms make it possible to take into account internal heat release in the material, which is especially important for calculations of future nanoelectronic circuits.

Using the above-introduced expressions for $\mathbf{q}$, κ_∞, and $\tau_R = \nu_R^{-1}$ and taking into account the estimate $\mu \sim l_N \langle v \rangle$, we reduce expression (14) to the following form:

$$\tau_R \frac{\partial \mathbf{q}}{\partial t} + \mathbf{q} = -\kappa_\infty \nabla T + l_N l_R \left(\nabla^2 \mathbf{q} + \frac{1}{3} \nabla (\nabla \cdot \mathbf{q}) \right). \quad (15)$$

Here, l_N and l_R are the mean free paths with respect to N-processes and the whole sum of processes of phonon-gas retardation in infinite medium, respectively. When a nonideal crystal is under study (i.e., when some other mechanisms of phonon scattering are taken into account along with U-processes), parameter l_R is applied instead of l_U. It is determined using the known Matthiessen formula $\tau_R^{-1} = \sum_i \tau_i^{-1}$; hence, $l_R = \tau_R v_S$, (v_S is the mean speed of sound).

In a general case, the Guyer–Krumhansl (GK) equations [21] have the following form. The energy conservation equation exactly coincides with Eq. (5). The quasi-momentum conservation equation somewhat differs from (15):

$$\tau \frac{\partial \mathbf{q}}{\partial t} = -\mathbf{q} - \kappa_\infty \nabla T + l_\infty^2 \left(\nabla^2 \mathbf{q} + 2 \nabla (\nabla \cdot \mathbf{q}) \right). \quad (16)$$

Thus, proceeding from different initial prerequisites, we obtained two equivalent equations (15) and (16).

Within the stationary approximation, taking into account energy conservation equation (5) without internal heat sources, expression (16) has the form

$$\mathbf{q} = -\kappa_\infty \nabla T + l_\infty^2 \nabla^2 \mathbf{q}. \quad (17)$$

Detailed derivation and analysis of the GK equations was given in [39].

The presence of the term $l^2 \nabla^2 q$ is common for the above forms of quasi-momentum conservation equations. This term within the Lifshitz–Pitaevskii approximation is obtained from the viscosity term in equality (13), which is similar to the Navier–Stokes equation. This indicates that the solution to these equations for thin films and nanowires has the form that is similar to the distribution of velocities obtained when analyzing Poiseuille flows in rarefied-gas flows of the corresponding geometries. However, there is no exact correspondence because of the above comparison of the motion equations for conventional and phonon gases. The coincidence is possible in the cases where the friction by walls exceeds the momentum loss determined by all the other processes.

Note that specifically the last term in (15) and (16) is responsible for the influence of small samples on the heat-transport character. It follows from (17) that the presence of the last term reduces heat flow in nanostructures in comparison with solids of large sizes under the same temperature gradients. In other words, the presence of the similar-to-viscosity term retards heat transfer. A decrease in the film thickness or nanowire diameter leads to a decrease in the effective thermal conductivity.

The GK system of equations is reduced to the differential equation with respect to temperature [39]:

$$\nabla^2 T + \frac{9 l_N}{5 \langle u \rangle} \frac{\partial}{\partial t} \left(\nabla^2 T \right) = \frac{3}{l_R \langle u \rangle} \frac{\partial T}{\partial t} + \frac{3}{\langle u \rangle^2} \frac{\partial^2 T}{\partial t^2}.$$

This is generalization of the classical heat-conduction equation, which includes this classical equation and hyperbolic wave equation (generally referred to as the Cattaneo–Vernotte equation) [45]. In the Soviet Union, this equation was derived somewhat later by Lykov. Furthermore, this equation contains an additional term including mixed time and space derivatives.

The models of nondiffusive heat transport, mathematically based on the GK system of equations, and with an equivalent but somewhat different approach developed in [24], were considered above.

The presented results give radically new knowledge about heat transfer in solids (in comparison with the generally accepted classical concepts). However, the processes providing heat transport in nano- and microstructures should be considered more completely. First, the problem of interaction between phonon gas and boundaries of a solid must be analyzed. Second, it is important to know how heat transport is implemented in a film or wire. These two factors determine the transport character on the whole. These problems were analyzed from different points of view in [23, 29, 39, 42, 43].

Let us first discuss the problem of interaction between the flow and boundary. It is studied based on two different approaches. One approach is analysis using the gas-dynamic model of heat transport. This approach calls for the formulation of correct boundary conditions for the phonon-gas flow at the boundaries. Different versions of boundary conditions and different functions were proposed for solving the system of equations [23, 39, 42, 43]. For example, the GK system of equations was used in [23]; therefore, the boundary condition is imposed on the heat-flow value q_W. As is known, the phenomenon of flow sliding at a wall occurs in rarefied-gas flows [46]. It was proposed in [39, 42, 43] to take into account flow sliding along the boundary. For example, the possibility of using the Maxwell formula was discussed in [39]:

$$v_W = CA \frac{\partial v}{\partial n},$$

and the more general formula

$$v_W = C_1 A \frac{\partial v}{\partial n} - C_2 A^2 \frac{\partial^2 v}{\partial n^2}.$$

Similar analysis was performed in [42, 43].

Furthermore, we will consider the kinetic approach to the problem of interaction between the phonon flow and boundary.

One of the first results on this important line of research was obtained in [26, 27]. The initial formula for determining thermal conductivity is the expression yielded by (7) and found in the solution of the Boltzmann equation [26] for macroscopic objects

$$\kappa_\infty = \left(\frac{k_B}{\hbar}\right)^2 \frac{k_B}{2\pi^2 V} T^3 \int_0^{\theta/T} \frac{\tau x^4 e^x}{(e^x - 1)^2} dx,$$

where $x = \hbar\omega/k_B T$ and V is the volume.

The processes of heat transport in nanowires were studied in [26]. The effective thermal conductivity is written as

$$\kappa_{eff} = \kappa_\infty - \Delta\kappa_{eff},$$

where $\Delta\kappa_{eff}$ is the correction taking into account the presence of phonon scattering at the nanowire boundaries. Omitting the corresponding formulas from [26], we note that in this model (as in the hydrodynamic model) the processes of interaction between phonon gas and boundaries are taken into account. More specifically, two types of phonon interactions with boundaries are taken into account. The first type is specular phonon reflection. The probability of this reflection type is assumed to be some value $p \le 1$. The second type is diffuse reflection with the probability $1 - p$.

Determination of the thermal conductivity requires calculation of relaxation time τ. The following processes of phonon scattering were taken into account in [26]: U-processes, phonon scattering by impurities with mass M, scattering at boundaries, and electron scattering. The corresponding times between collisions are calculated for each of these processes: τ_U, τ_M, τ_B, and τ_{ph-e}. According to the Matthiessen rule, the desired time is $\tau^{-1} = \tau_U^{-1} + \tau_M^{-1} + \tau_B^{-1} + \tau_{ph-e}^{-1}$. Quantum confinement, which is significant in the cases where phonon wavelengths are comparable with the wire diameter, was also taken into account. As is known, this effect reduces the wave group velocity and, accordingly, thermal conductivity. The dependences $k_{eff}(T)$ and $k_{eff}(p)$ were calculated. At 300 K, the thermal conductivity is more than 150 W/(m K) for a macroscopic silicon sample, whereas, for a nanowire 20 nm in diameter, taking into account the above factors, the thermal conductivity at $p = 0$ is about 15 W/(m K). Analysis of the dependence $k_{eff}(p)$ showed that the increase in p leads to an increase in k_{eff} (this is obvious). However, the transition to $p = 1$ does not provide coincidence with k_∞ because of the influence of quantum confinement. For $p = 1$, the thermal conductivity is 110 W/(m K) at 300 K.

In [47], the analysis was also performed based on the kinetic theory. Here, investigation of the problem is focused on statistical analysis of interactions between quasiparticles and the boundary. The probability p of specular phonon scattering at the boundary surface is also introduced. It was revealed that the condition $l_\infty \gg L$ does not ensure ballistic transport. The reason is the same as in the previous example. Furthermore, parameter p in the used approximation is not constant but depends on roughness η (nm). According to Soffer [48], this relationship has the form $p(k) = \exp(-4k^2\eta^2)$. It is clear that the thermal conductivity decreases with an increase in η and vice versa. Thus, not only the size of the sample but also the quality of its surface affects the thermal conductivity.

The next important problem is to determine fractions of the ballistic and diffusive regimes in the total heat transport. This question was considered in detail in [47]. The consideration is based on the kinetic theory. The expression for thermal conductivity is in fact the same as that yielded by the solution of Boltzmann equation (6):

$$\kappa_{eff} = \frac{1}{(2\pi)^3} \sum_j \int k_B (\hbar\omega_j/k_B T)^2 \times \frac{\exp(\hbar\omega/k_B T)}{[\exp(\hbar\omega/k_B T) - 1]} u_j(\mathbf{k}) l_j(\mathbf{k}) \mathrm{Cos}^2\theta d\mathbf{k}. \quad (18)$$

The structure of this formula is the same as (7): there is the product of specific heat, mean speed of sound, and mean free path under the integral. However, the fundamental difference is that l_∞ is used as the mean free path in (6), whereas in formula (18) parameter $l_j(\mathbf{k})$ is used, which takes into account interactions with phonons and scattering at boundaries and lattice irregularities. Therefore, the expression for $l_j(\mathbf{k})$ considers all these factors [49]. As a result, thermal conductivity is calculated taking into account the shape and sizes of the body under study. In [47], this body was a silicon nanowire.

The analysis begins with the regime where interactions of phonons inside the body can be neglected (i.e., when they are scattered only at the boundaries). This is the purely ballistic heat-transport regime (the so-called Casimir limit). It is interesting that there are hardly any N- and U-processes in this regime. According to the above-said, the condition $\mathrm{Kn} = l_\infty/L \gg 1$ is not a rigorous criterion for ballistic transport. The more accurate expression is [47]

$$1 - \exp(-L/l_\infty) \cong \mathrm{Kn}^{-1} \ll 1 - p.$$

The most important factors determining the ballistic heat-transport regime are the sample size (nanow-

ire diameter, film thickness, or nanotube length), temperature, and surface roughness. Furthermore, we present calculations of thermal conductivity κ from formula (18) at specified p and η values in the ranges of temperatures T from 0 to 300 K and nanowire diameters d from 10 nm to 1 μm. Casimir thermal conductivity κ_C is simultaneously calculated using the specially determined Casimir mean free path $l_C(\mathbf{k})$. The results of these calculations allow one to determine the ratio $\kappa_C/\kappa(d,T,p,\eta)$, which is a fraction of ballistic transport in the total heat flow. The ratio $\kappa_F/\kappa(d,T,p,\eta)$, which is a fraction of diffusive transport in the total heat flow, is determined in a similar way. We present a numerical example of the calculations. At a given roughness of $\eta = 0.2$ nm, ballistic transport occurs at $T < 140$ K when $d \le 10$ nm and at lower temperatures ($T < 20$ K) when $d \le 10$ μm.

Thus, the quite complete analysis of heat transfer in nanostructures is not reduced to the solution of one system of equations but requires comprehensive study.

The models of non-diffusive heat transport, mathematically based on the GK system of equations, and equivalent but somewhat different approach developed in [24] were considered above.

Recently, a new approach has been proposed, the results of which are similar to the GK model concerning the mathematical content and calculated data. Nevertheless, it is of independent interest [45, 50]. The results obtained in these and some other studies were referred to therein as the thermal-mass model. This name indicates that authors proceeded from the conventional hydrodynamics for media consisting of particles with a finite mass. This was achieved due to the Einstein relation $E = mc^2$. As the gas-dynamic model, this model is macroscopic. Thermal conductivity is modeled by a gas having mass density and flowing through a porous medium. A change in the mean free path l_R is interpreted as the change in the porosity of the medium, whereas a change in l_N is due to the change in viscosity. A set of calculation data was obtained based on this theory which is well consistent with experimental [32, 51] and calculation data found proceeding from some other results [52].

Another approach was formulated in [53], where the separate expressions for the kinetic (diffusion), κ_{kin}, and collective (hydrodynamic), κ_{coll}, components of the total thermal conductivity κ were obtained. These three values are related by the following expression:

$$\kappa = \kappa_{kin}(1 - \Sigma) + \kappa_{coll}\Sigma,$$
$$\Sigma = \tau_R/(\tau_R + \tau_N).$$

The models describing longitudinal heat transport in nanostructures were considered above. Below, we will briefly discuss the models that were developed for determining characteristics of transverse heat transport. One of the first related studies is [30], which was based on the solution of the Boltzmann equation. The distribution function is assumed to consist of two parts: ballistic and diffusive. The ballistic part includes phonons moving in a certain direction from one boundary (with which they have collided) to the other. The remaining phonons enter the diffusive part (the phonons that were created or scattered at internal points of the sample).

A model of transverse heat transport was proposed in [34], which is based on the use of the Boltzmann equation. The collision term of the equation is taken in the form

$$St(N) = -\frac{N - N_E}{\tau_R} - \frac{N - N_D}{\tau_N}.$$

Here, the first term takes into account phonon scattering, while the second term takes into account N-processes. As a result of the solution, we determine deviations from the equilibrium functions N_E and N_D, which have the form

$$N_E = \frac{1}{\exp\left(\frac{\hbar\omega}{k_B T}\right) - 1}, \quad N_D = \frac{1}{\exp\left(\frac{\hbar\omega - \hbar\mathbf{ku}}{k_B T}\right) - 1}.$$

A radiative phonon model was proposed for studying ballistic heat transport [8]. The essence of this model is as follows. The formulas for equilibrium radiation of planes that limit the nanofilm and have different temperatures are written. In contrast to conventional problems of electromagnetic-wave radiation, the Planck function is integrated from zero to ω_{max}.

RESULTS OF THE NUMERICAL CALCULATIONS

Let us first consider how the problems of heat transfer are stated for macro- and nanoobjects.

In the cases where the condition $\mathrm{Kn} = l_\infty/L \ll 1$ is satisfied (i.e., when the Fourier approximation providing classical diffusive heat transport is applicable), the main theoretical problem is to determine thermal conductivity κ_∞ for specified microscopic structure of material. For a certain material, this parameter depends on temperature but is independent of the geometric characteristics of objects made of this material. When the approximation of smallness of the number Kn is not satisfied (i.e., $\mathrm{Kn} > 1$), the problem is to determine effective thermal conductivity κ_{eff} under the following conditions. First, as in the case of $\mathrm{Kn} \ll 1$, microscopic structure of the material is given. Second, one should specify the shape of the nanosized solid. Third, the sizes of this solid should be set. Fourth, it is important to take into account the heat-flow direction because the properties of nanostructures are anisotropic even at ideal isotropy of the microscopic structure. According to the calculation

results [13], the degree of anisotropy of a single-crystal nanofilm can be as high as 1.8. For nanotubes, it is important to indicate the chirality (i.e., position of hexagonal cells with respect to the system axis) and whether the tube is single-wall or multiwall.

The aforesaid means that, in the general case, the problems related to studying heat propagation in the range $\mathrm{Kn} \geq 1$ are more diverse than those for the range $\mathrm{Kn} \ll 1$. As a result, there are many different models describing heat transport in such systems.

In the relatively simple case of thin films, the influence of the size can be estimated by taking into account that the classical thermal conductivity is proportional to the mean free path. Then, for example, if $\mathrm{Kn} \gg 1$, we can assume that $l(\mathrm{Kn} \gg 1) \cong L$. As a result, we have $\kappa_{\mathrm{eff}}/\kappa_\infty \cong (\mathrm{Kn})^{-1}$. In the region of intermediate Knudsen numbers, such estimation gives

$$\frac{\kappa_{\mathrm{eff}}}{\kappa_\infty} = \frac{1}{1+\mathrm{Kn}}. \qquad (19)$$

Currently, there are several such simple relations concerning different domains of definition of Kn [31]. However, they do not take into account the heat propagation direction. One should bear in mind that thermal conductivity of a nanofilm of a fixed thickness differs significantly for longitudinal and transverse heat flows [13]. Therefore, the use of such estimations yields rather rough results.

Theoretical predictions presented in the previous sections require experimental confirmation, and the experimental data should be compared with the results of numerical calculations. First of all, one should check in the initial analysis stage if the effective thermal conductivity indeed depends on the sample sizes. Generally, the case in point is sample sizes on the order of the phonon mean free path or smaller. As was noted above, the mechanism of heat conduction under these conditions radically differs from classical diffusive heat conduction based on the Fourier law. It is important to determine the effective thermal conductivity in longitudinal and transverse directions (for example, if a nanofilm is under study).

Below, we will very briefly consider the main methods of calculating the effective thermal conductivity, which are currently most widely applied.

The first one is the molecular dynamics (MD) method. It is very popular. Accordingly, many interesting results were obtained using it. The dynamics of lattice of a solid is studied within this method. The system of Newton equations is written for each lattice atom. However, this method has two significant drawbacks. One of them is high laboriousness, due to which the results for rather large samples are difficult to obtain; however, the main drawback of the method is that the lattice is described using classical mechanics, whereas the whole theoretical base of thermodynamics and heat transfer in solids is based on the Bose–Einstein quantum statistics. When analyzing processes in a solid, one should use Bose–Einstein quantum statistics (2): $N_0 = 1/[\exp(\hbar\omega/k_\mathrm{B}T) - 1]$. In the classical limit (when the body temperature exceeds significantly the Debye temperature $T \gg \theta_\mathrm{D}$ and, correspondingly, $\hbar\omega/k_\mathrm{B}T \ll 1$), this relation yields $N_0 = k_\mathrm{B}T/\hbar\omega$. Here, the energy of most phonons is $\hbar\omega \sim k_\mathrm{B}\theta_\mathrm{D}$. In these limits, the MD method can be used. As can be seen, this consideration is valid for sufficiently high temperatures (higher than the Debye temperature for the corresponding material θ_D). It is known that for most materials the Debye temperature is lower than 300 K or slightly exceeds this value [8]; however, $\theta_\mathrm{D} = 2000$ K for carbon. Therefore, the use of the MD method and classical approximation may lead to errors when estimating thermal conductivity [36, 54, 55].

Thus, the calculation results for sufficiently high temperatures (for example, from 300 to 1000 K for silicon) can be accepted.

The second approach is based on the use of the Boltzmann kinetic equation for heat carriers (phonons). In this case, the solution is performed using quantum-mechanical methods. The initial distribution is the Bose–Einstein energy distribution for phonons. Thermal conductivity is determined as a result of summation over the contributions from different polarizations. The polarization is considered to be a wave type. Generally, one deals with acoustic low-frequency waves *LA* and *TA*. This makes it possible to determine relative contributions from different polarizations to heat transfer in corresponding objects. The solution is performed within the linear approximation.

The approximation of the nonequilibrium Green function is fairly effective for studying heat conduction of nanostructures. This method was developed for nonequilibrium Fermi systems by L.V. Keldysh [24] and then for phonon gas in [56, 57]. This method allows one to find the exact solution from the first principles taking into account the quantum-mechanical nature of phonon gas.

The Monte Carlo method was used in some studies for calculating thermal conductivity of nanostructures [58, 59].

Let us first consider the studies, in which the dependences $k_{\mathrm{eff}}(L)$ for nanotubes were investigated.

Numerical analysis of ballistic heat conduction in a carbon nanotube was carried out in [36]. The tube chirality was not indicated. The investigation was performed based on the solution of the Boltzmann equation (Boltzmann–Peierls equation, according to the terminology accepted by the authors) taking into account finite nanotube size L. As a result, two dependences of the effective thermal conductivity on the tube length were obtained. One dependence,

$$\kappa_{\text{eff}} = AL^{1/2},$$

corresponds to the conditions where linear dispersion relations (i.e., Debye approximation) occur. If there is a quadratic dependence of the frequency on the wave vector occurs (which is typical, for example, of bend oscillations [37]), the corresponding dependence has the form

$$\kappa_{\text{eff}} = AL^{1/3}.$$

The dependences of the effective thermal conductivity on the length of a single-wall carbon nanotube were calculated in [60] by the MD method for two diameter values and identical chirality: (5, 5) and (10, 10); temperature is 300 K. It was shown that, for the tube (5, 5), the dependence has the form $k_{\text{eff}} = AL^{0.32}$ in the range of L from 6 to 404 nm. Notably, k_{eff} changed from 160 to 600 W/(m K). For the sample (10, 10), thermal conductivity changed only slightly in the above range of tube lengths. The results obtained yield thermal conductivity that is much lower as compared with MD calculations for large samples. In the latter case, the nanotube thermal conductivity is 1000 W/(m K) or higher [61].

Note that such power-law dependences $k_{\text{eff}}(L)$ are valid only in relatively narrow ranges of variation in L. The dependence $k_{\text{eff}}(L)$ that approximately corresponds to (19) is applicable in the entire range from almost zero to the values, at which diffusive heat transport is implemented (i.e., k_∞).

Thermal conductivity of nanotubes was numerically investigated in [55] by the MD methods. In particular, the influence of the chirality on the thermal conductivity at a fixed tube length and 300 K was studied. Calculations showed that this influence is weak. The tubes of (9, 0), (10, 0), and (5, 5) were considered. The thermal-conductivity values varied in the range 3–5%. The tube radii were 0.357 nm for (9, 0) and 0.397 nm for (10, 0). Moreover, the influences of the tube length and temperature were studied. For the tube of (5, 5) and at 300 K, the tube length was varied from 2 to 10 nm. The thermal conductivity increased from 200 to 3000 W/(m K). Accordingly, the effective thermal conductivity depends on the tube length as $\kappa_{\text{eff}} = AL^{0.40}$. The thermal conductivity of the same tube at 800 K increases from 400 to 800 W/(m K) with a change in the length from 10 to 100 nm. In this case, the following dependence was obtained: $\kappa_{\text{eff}} = AL^{0.26}$. For the tube of (10, 10), we have $\kappa_{\text{eff}} = AL^{0.38}$ at 300 K and $\kappa_{\text{eff}} \infty L^{0.12}$ at 800 K. Thus, the dependences $\kappa_{\text{eff}}(L)$ significantly differ from each other at high temperatures and different chirality values.

The dependences of the thermal conductivity of carbon and boron nitride nanotubes were calculated in [32] based on the system of equations obtained by the authors within the thermal-mass model. The carbon tube was 1.65 nm in diameter and 3.02 μm in length. The boron nitride tube sizes were 10 nm and 5 μm, respectively. It was shown that the thermal conductivity increases for both materials. The carbon-tube thermal conductivity increases from 50 to 300 W/(m K) in the range of 50–500 K. The thermal conductivity of the boron nitride tube increases from 50 to 350 W/(m K) in the range of 50–300 K. The calculation results are in very good agreement with the experimental data.

Let us now consider some results of calculating thermal conductivity of nanofilms. Note that the thermal conductivity of nanofilms is different for longitudinal and transverse directions. The heat-transport mechanisms also differ. In the case of longitudinal heat transport, the retardation of heat transfer is mainly due to the phonon scattering at boundaries. The thermal conductivity naturally increases with an increase in the film thickness. For transverse heat transport, the thermal conductivity also grows with an increase in the film thickness because the mean free path increases.

GK system of equations (15) was used in [23] for analyzing longitudinal heat conduction. The following analytical solution was obtained:

$$\frac{\kappa_{\text{eff}}}{\kappa_\infty} = 1 - \frac{\tanh(0.5\text{Kn}^{-1})}{1 + 0.5\text{Kn}}.$$

It follows from this expression that $\kappa_{\text{eff}} = \kappa_\infty$ for $\text{Kn} \ll 1$. For $\text{Kn} \gg 1$, $\kappa_{\text{eff}} \to 0$, which is invalid because this is the case of ballistic heat conduction. The solution obtained is in qualitative agreement with the experimental data obtained by some researchers. Interesting data on thermal conductivity of nanowires were presented in [62].

The authors of [38] used the gas-dynamic approximation and, correspondingly, GK system of equations (15) to determine the longitudinal thermal conductivity of a film. The condition taking into account phonon-gas flow sliding at a wall was used as the boundary condition at the wall:

$$V_S = Cl_\infty \left(\frac{\partial V(z)}{\partial z}\right)_{z=L/2}.$$

Here, V_s is the gas velocity at the film surface, C is a constant characterizing the value of gas sliding at the film surface, and L is the film thickness. The result of the analytical solution of the GK system of equations has the form

$$\frac{\kappa_{\text{eff}}(l_\infty/L)}{\kappa_\infty} = \frac{1}{12}\left(\frac{L}{l_\infty}\right)^2 \left[1 + 6C\frac{l_\infty}{L}\right].$$

Depending on the ratio between two terms in the square brackets, this dependence is proportional in limiting cases to the (L/l_∞) ratio in either the second or first power. Note that the power-law dependences

$\kappa_{eff}(L)$ were obtained for the first time by Gurzhi in 1968 [19]. It is interesting that his results exactly coincide with those presented here. However, such dependences do not ensure correct κ_{eff} values in limiting cases.

The results of calculating the longitudinal and transverse thermal conductivities of a silicon nanofilm were presented in [34]. The longitudinal thermal conductivity was determined using the momentum conservation equation from the thermal-mass theory

$$\frac{l_R(z)}{l_{R\infty}}\kappa_\infty \nabla T = -q(z) + \frac{l_R(z)l_N(z)}{5}\nabla^2 q(z).$$

Here, z is the axis oriented normal to the film symmetry plane with the coordinate origin on this plane.

The transverse thermal conductivity is determined by solving Eq. (19). The obtained values vary from 5 to 140 W/(m K) with a change in the film thickness from 1 to 100 nm. The ratio of the transverse thermal conductivity to the longitudinal changes from 1.84 to 1 with a change in the film thickness from one to thousand nanometers.

Unfortunately, as in the other mentioned studies, the temperature, for which the calculations are performed, was not reported.

Below, we will consider the results of numerical investigations of heat transport in nanowires. A series of calculations of the nanowire thermal conductivity in the range from 1 nanometer to 100 μm were carried out in [62]. The calculations were performed using the solution of the Boltzmann equation for thermal conductivity with phonon scattering at boundaries accurately taken into account (see also [47] for nanofilms). The following results were obtained. The dependences of the thermal conductivity of nanowire on its diameter were obtained within the approximation of constant probability p of specular phonon scattering at the wire surface. The p values of 0.0, 0.5, and 0.9 were taken. The obtained dependences are similar to the dependences for nanofilms depending on their thickness. The diffusive regime of heat conduction occurs at the wire diameter of ≈100 μm.

In addition, calculations of the so-called cumulative (accumulated) thermal conductivity were also carried out in this study. The results of these calculations descriptively show the contributions from different portions of the phonon spectrum to the resulting thermal conductivity. The calculations were performed for temperatures of 20, 50, and 300 K. It was shown, for example, that these dependences at 300 K almost coincide for the diameters of 10 nm, 100 nm, and 1 μm. Furthermore, more than 90% of heat transfer occurs in the wavelength range from about 1 to 10 nm. For temperatures of 50 and 20 K, 90% contribution to the thermal conductivity is obtained in the phonon wavelength range up to 30 and 40 nm, respectively.

Thermal conductivities of ten semiconductors (AsGa, InP, AlSb, GaSb, InAs, InSb, ZnS, ZnSe, ZnTe, and CdTe) were calculated in [63] at 300 K in the wire diameter range from 30 nm to 10 μm. The authors obtained some generalized dependence for these materials at the nanowire diameter of 30 nm:

$$\frac{\kappa}{\kappa_\infty} = (1+r)^{3/2}.$$

Here, $r = M_l/M_h$, M_l is the smaller mass of elements entering the semiconductor, and M_h is the larger mass.

An analytical solution for κ_{eff} as applied to nanowires was obtained in [23] based on the GK system of equations. It has the form

$$\frac{\kappa_{eff}}{\kappa_\infty} = 1 - \frac{4\mathrm{Kn}^2 I_1(0.5\mathrm{Kn}^{-1})}{1+\mathrm{Kn}I_1(0.5\mathrm{Kn}^{-1})}.$$

SOME EXPERIMENTAL DATA ON THE PROCESSES OF NONDIFFUSIVE HEAT TRANSFER

Phenomena of nondiffusive heat transfer in solids were theoretically predicted long ago [18, 19, 64]. The main analytical expressions that relate κ_{eff} with T and characteristic size L were obtained in these studies for the first time. However, the complexity of the corresponding processes induced a need in not only experimental confirmation of these phenomena but also comprehensive analysis of the influence of geometry, chemical and phase compositions, and some other structural features of objects on the heat-transfer efficiency therein.

To date, investigations of heat transfer in low-temperature (with $T \le 10$ K) crystalline cylindrical samples of helium ^{4}He [65, 66], bismuth Bi [20], parahydrogen [67, 68], and germanium ^{70}Ge [69, 70] have been performed. First, we note some specific features of the κ_{eff} behavior depending on T and L. Samples diameters d_0 were chosen to be L. It was shown that the temperature dependences of κ_{eff} are nonmonotonic and have a maximum $\kappa_{eff}^{(max)}$ at temperature T_m (see Table 1). In relatively narrow ranges of T and L, the κ_{eff} value can be approximated by the function $\kappa_{eff} \propto T^n L^m$, where n and m are constants. It was noted that n depends significantly on the ratio between T and T_m. For example, the values of $n \approx 3$ [65–68] and $n \approx 3.5$ [20] were observed experimentally for various materials at $T \ll T_m$, whereas at $T \le T_m$ the following values were obtained: $n \approx 6$–8 [65, 66, 69, 70], $n \approx 4.5$–10 [67, 68], and $n \approx 3.5$ [20]. The m values for Bi at $T \le T_m$ were found to be ≈1.2–1.4 [20]. At $T > T_m$, κ_{eff} passes through extremum and gradually decreases. In the limit $T \gg T_m$, differences in the behavior and

Table 1. Some results of experimental studies on heat transfer in cylindrical (length l_0, diameter d_0) crystalline materials at low temperatures

References	Measurement technique	Material	l_0, cm	d_0, cm	T_m, K	κ_{eff}, kW/(m K)	$l_{eff}(T_m)$, cm
[20]	Stationary thermo- and calorimetry	Bi	below 8	0.15–0.51	3–4	1–3	–
[65, 66]		He	5.2	0.25–0.6	0.8–1.2	2–5	0.2–0.7
[67, 68]		Parahydrogen	–	0.6	3–4	3–4	0.15–0.32

numerical values of $\kappa_{eff}(T)$ disappear for all the investigated materials.

Thus, one can separate three main regions in the $\kappa_{eff}(T)$ behavior depending on temperature; these regions differ significantly by the characteristic phonon mean free paths in *N*- and *U*-processes, which depend on temperature [18–20, 67, 68] as $l_N \propto (T/\theta_D)^5$ and $l_U \propto \exp(\theta_D/T)(T/\theta_D)^{5/2}$. In the case of extremely low temperatures, $T \ll T_m$, the ballistic heat-transfer regime is implemented, in which l_N and l_U exceed significantly the characteristic object size L. In this case, the effective phonon mean free path is determined by the characteristic size of the sample: $l_{eff} \approx L$. Thus, the scattering occurs only at the boundaries of the material. The following theoretical formula is valid for κ_{eff} in the ultralow-temperature limit: $\kappa_{eff} \propto T^3 L$ [18, 19, 64]. When the temperature increases to $T \leq T_m$, the phonon-gas motion regime changes to hydrodynamic, for which the two-sided inequality $l_N < L < l_U$ is valid and *N*-processes with quasi-momentum conservation dominate. Here, l_{eff} is determined as the distance, which the colliding phonons pass from one sample boundary to the other (i.e., $l_{eff} \approx L^2/l_N$) [18, 19]. In this case, the theory [18, 19] yields $\kappa_{eff} \propto T^8 L^2$, and the numerical κ_{eff} values are larger than those for the ballistic regime by a factor of 10–15. With a further increase in temperature to $T > T_m$, the l_N and l_U values significantly decrease in comparison with L ($l_N < l_U < L$) [20] and the phonon motion is limited by *U*-processes, and $l_{eff} \approx l_U$. While l_U decreases, this circumstance gradually leads to a decrease in κ_{eff}. The process of heat transfer becomes diffusive.

To confirm the phenomenon of hydrodynamic phonon heat transfer, the dependence of the effective phonon mean free path $l_{eff}(T)$ on temperature was estimated in [20, 67, 68] based on the known dependences $\kappa_{eff}(T)$ and compared with the corresponding dependence on L. It was shown that $l_{eff}(T)$ increases with a decrease in temperature, levels off to the plateau $l_{eff}^{(max)} \propto L$ at $T = T_m$, and barely changes at a further decrease in temperature. The characteristic $l_{eff}^{(max)}$ values may reach 0.15–0.7 cm [20, 67, 68]. This indicates that at $T \leq T_m$ the only process limiting the heat-transfer efficiency is phonon scattering at the sample boundaries. Proceeding from this circumstance and the fact that the experimental dependences $\kappa_{eff}(T, L)$ are in satisfactory agreement with the theoretical data of [18, 19, 64], the authors of [20, 67, 68] made a suggestion that the hydrodynamic phonon-motion regime can be implemented in the investigated objects at $T < T_m$.

It is interesting that the absolute κ_{eff} values strongly depend on the existing impurities and structural defects. For example, the κ_{eff} value for ^{70}Ge crystals with the degree of purity of 99.99% is larger by a factor of 2.5–3.0 than that for ^{70}Ge with the degree of purity of 96% at an identical temperature [69, 70]. This is caused by the efficient (for the more contaminated sample) phonon scattering from impurities.

The possibility of deviation from the diffusive mechanism of heat propagation in solids of small sizes (comparable with the phonon mean free path) was predicted for the first time in [71]. The influence of roughness on the heat transport in the cases where the scattering at boundary surfaces of small samples is significant was also discussed in this study (see also [48]). These objects include [72], for example, nanotubes, nanowires, thin films, superlattices, etc. For a long time, investigation of the thermal properties of such systems has been difficult because of the absence of corresponding techniques. However, currently the number of studies on this line of research constantly increases due to the development of the experimental techniques [3].

It should be noted that heat transport in small-size objects (with the characteristic sizes of no more than 10 μm) differs from that in bulk objects of the same chemical composition. The thermal properties of bulk crystalline solids are mainly isotropic. However, this does not hold true for small-size objects, where anisotropy of κ_{eff} is caused by anisotropy of l_{eff} due to the significant difference between the object sizes, structural features, etc. [73]. Therefore, it is customary for thin films, for example, to separate the transverse (across their surface area), $\kappa_{eff\perp}$, and longitudinal (along the surface area), $\kappa_{eff\parallel}$, effective thermal conductivities. Notably, the experimental techniques for

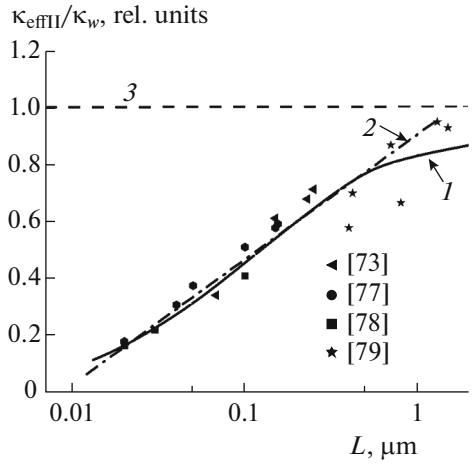

Fig. 1. Comparison of the experimental data on the dependence $\kappa_{eff||}/\kappa_\infty$ for silicon films on their thickness L [73, 77–79] with (*1*) theory [82] and dependences for the (*2*) ballistic, $\beta \approx 1$, and (*3*) diffusive, $\beta \approx 0$, regimes of heat transfer.

determining these values may differ significantly [40, 73, 74].

In one of the earlier experimental studies [40], the transverse thermal conductivity of thin SiO_2 films with a thickness of 10^{-2}–1.0 μm was investigated by calori- and thermometry methods from 300 to 460 K. The films were prepared by thermal oxidation of Si substrates. Doped SiO_2 films containing 3.0% B and 4.5% P were synthesized by chemical vapor deposition to analyze the influence of impurities on $\kappa_{eff\perp}$. It was experimentally shown that $\kappa_{eff\perp}$ depends on the characteristic size L (film thickness in this case) as $\kappa_{eff\perp} \propto L^\beta$, where β is constant, which was not determined numerically in the study. The authors believed this dependence of $\kappa_{eff\perp}$ on L is caused (as in [20, 65–68]) by the surface phonon scattering at the Si–SiO_2 interface and the influence of this scattering on the heat-transfer efficiency. The characteristic $\kappa_{eff\perp}$ values for the investigated films were 4×10^{-3}–0.5 W/(m K) (at 373 K), which is much lower than the thermal conductivity of a bulk quartz sample: $\kappa_\infty \approx 1.38$ W/(m K) [75]. It was established that $\kappa_{eff\perp}$ for the doped films is smaller than that for the undoped SiO_2 sample by a factor of 2.0–3.0 because of the additional volume phonon scattering from impurities. It was experimentally shown that temperature affects $\kappa_{eff\perp}$ for thin SiO_2 films. For example, the $\kappa_{eff\perp}$ values decrease by a factor of 1.5–2.0 with an increase in temperature from 300 to 460 K.

The development of microprocessor technology required thorough investigation of the heat-transfer processes in thin semiconductor films deposited on dielectric substrates. These objects include thin Si films on SiO_2 wafers, which are referred to as silicon on insulator (SOI) [76]. A number of studies [73, 77–80] were devoted to thermal properties of such objects, in which the longitudinal thermal conductivity $\kappa_{eff||}$ of Si films was investigated.

The behavior of $\kappa_{eff||}$ for silicon films with thickness $L = 0.02$–1.6 μm in SOI (SiO_2 layer thickness is about 3 μm) was analyzed in [77–80] using calorimetry methods at 20 to 350 K. In these studies, stationary sample heating by Joule's heat was applied and temperatures were measured at different points of the samples using heat resistances. As a result, the law of change in temperature [81] along the film surface was determined, which was used to calculate $\kappa_{eff||}$. Some techniques have recently been developed, which are based on contactless determination of the dynamics of thermal fields in Si membranes and films by the methods of laser-induced nonstationary thermal gratings [74] and thermal-reflection measurement [73]. These methods are based on nonstationary heating of objects with subsequent laser probing of their surfaces and analysis of the laser-radiation characteristics. These diagnostics techniques (in contrast to the above-considered contact methods) yield information about the dynamics of heat processes in thin Si films.

Having summarized the data of [77–80], we should note that there is deviation from the diffusive heat transfer for almost all thin Si films investigated in these papers. The degree of this deviation (quantitatively expressed as the $\kappa_{eff||}/\kappa_\infty$ ratio) is mainly determined by the thickness and temperature of the film. Figure 1 shows experimental points of the dependence $\kappa_{eff||}(L)/\kappa_\infty$ at room temperature and the corresponding data obtained from theoretical estimations [82]. It was shown that the theory is fairly well confirmed by the experiment for almost all considered L values. The estimations predict rather complex behavior of $\kappa_{eff||}(L)$. This indicates that the dependence $\kappa_{eff||}(L) \propto L^\beta$ should be considered as a piecewise-specified one, and the β values are determined by film thickness L. Thus, the cases of $\beta \approx 1$ and $\beta \approx 0$ can be considered as examples of, respectively, ballistic and diffusive mechanisms of heat transfer. In this context, we can state that at $L <$ 1.0 μm (see Fig. 1) and room temperature the heat-conduction efficiency is limited almost entirely by phonon scattering at the boundaries of a solid, and the energy-transfer process is ballistic.

The found dependence $\kappa_{eff||}(L)$ makes it possible to estimate the effective phonon mean free path as $l_{eff||} \approx 1.0$–2.5 μm (under standard conditions). It was proposed in [74] to consider $l_{eff||}$ as the mean free path of low-frequency phonons, because specifically they are characterized by maximum values. It was noted that these estimates exceed significantly $l_{eff||} \approx 0.04$ μm, a value determined based on the simple gas-kinetic theory [83], in which the contribution from phonons of this type was neglected. As analysis showed [74], there

Table 2. Some results of experimental studies on longitudinal thermal conductivity $k_{\text{eff}\parallel}$ of thin silicon films with thickness L

References	Measurement technique	L, μm	T_m, K	$k_{\text{eff}\parallel}^{\max}$, W/(m K)	$l_{\text{eff}}(T \approx 300\,\text{K})$, μm	β
[73]	Thermal-reflection measurement	0.068–0.258	–	–	~2	0.564
[74]	Laser-induced nonstationary thermal gratings	0.4	–	–	~1.0–2.5	–
[78]	Stationary thermo- and calorimetry	0.02–0.1	100–110	20–100	~1	0.558
[79]		0.42–1.6	70–100	110–130	~1	0.306

is only scarce quantitative information about the influence of structural features (impurities, defects, etc.) on $l_{\text{eff}\parallel}$ and, accordingly, the efficiency of heat transfer as a whole.

Studies [77–80] made it possible to establish the specific features of the influence of temperature on $\kappa_{\text{eff}\parallel}$. It was shown that the qualitative behavior of $\kappa_{\text{eff}\parallel}(T)$ is also nonmonotonic (as in the above-considered case of bulk samples at low temperatures). It is interesting to note that, in contrast to bulk crystalline solids at low temperatures for which the ballistic heat-transfer regime is implemented at $T \ll T_m$ [18, 19], in the case of the considered thin Si films, these phenomena may occur at $T \geq T_m$ as well. As was noted above, this is due to the fact that their thickness is sufficiently small to satisfy the condition $l_N < L < l_U$. To compare the data obtained by different authors, the T_m, $\kappa_{\text{eff}\parallel}^{(\max)}$, $l_{\text{eff}\parallel}$ and β values for thin Si films at room temperature are listed in Table 2. It was shown that for Si films with thickness $L \approx 0.02$–1.6 μm the maximum of $\kappa_{\text{eff}\parallel}^{(\max)} \approx 2.0$–130 W/(m K) is observed at $T_m \approx 70$–110 K. The β values were determined by processing the data of [73, 77–79].

Description of another promising method of analyzing heat-transfer processes in thin metal films and the obtained results were presented in [84]. Heat conduction of the system composed of thin nickel strips (width 0.02 μm, length 0.12 μm, and thicknesses L from 0.065 to 2 μm), deposited parallel to each other by electron lithography on transparent sapphire or fused 0.8-μm-thick silica substrates, was investigated in this study. This method is based on determination of thermal resistances of two-layer (metal film–dielectric substrate) systems by investigating specific features of the dynamics of surface acoustic waves arising in metal films upon their pulsed laser heating.

The transverse coefficients of thermal resistance were determined in [84] based on the mathematical processing of experimental results. It was shown that the substrate material affects significantly the heat-transport characteristics. A small deviation from the Fourier law is observed for the quartz-glass substrate at $L \leq 0.1$ μm, whereas for the sapphire substrate it is pronounced at larger L values ($L \leq 1.0$ μm). The authors related this behavior of the thermal resistance to the significant difference in the phonon mean free paths in fused silica ($l_{\text{eff}\perp} \approx 0.02$ μm) and sapphire ($l_{\text{eff}\parallel} \approx 0.12$ μm). Note that this work does not contain analysis of the influence of the thickness of the substrate, its surface roughness, and other parameters on the deviation from diffusive heat transfer. In addition, the experimental results were processed using macroscopic thermophysical parameters (specific heat, thermal-expansion coefficient, etc.), which may significantly differ for thin films and bulk samples of Ni.

Recently, many experimental studies [85–87] on heat transfer in nanowires have been performed for different applications [72].

The data on thermal conductivity of Si and Ge nanowires obtained by microcalorimetric methods were presented in [85–87]. In these studies, nanowire diameters d_0 were chosen as the characteristic size L; these values were $L \approx 0.01$–0.115 μm at length l_0 of several micrometers. Temperature in the experiments was varied from 20 to 320 K. Behavioral features of the dependence of k_{eff} on T and L for Si nanowires were established in these works. It was shown that the relation $\kappa_{\text{eff}} \propto T^3$ is valid for the diameters from 0.056 to 0.115 μm at low temperatures ($T \approx 20$–60 K), which is in agreement with the theory [18, 19, 64]. When the nanowire diameter decreases to $d_0 \approx 0.022$–0.037 μm, there are a deviation from the Debye theory and a dispersion of values from $\kappa_{\text{eff}} \propto T$ to $\kappa_{\text{eff}} \propto T^2$. As was noted in [85], this circumstance can be due to the specific features of phonon–phonon scattering and some other effects that are significant on such scales. The experiments showed that the κ_{eff} values for the considered wires are about two orders of magnitude smaller than those for a bulk sample, which is caused by the higher efficiency of boundary phonon scattering [47]. The theoretically predicted thermal conductivities of nanowires [88] are in good agreement with the above experimental data.

Interesting objects are nanowires with heterogeneous interface [87]. These structures are composed of, for example, Si core of round cross section with a diameter of 0.012–0.045 μm surrounded by a Ge shell

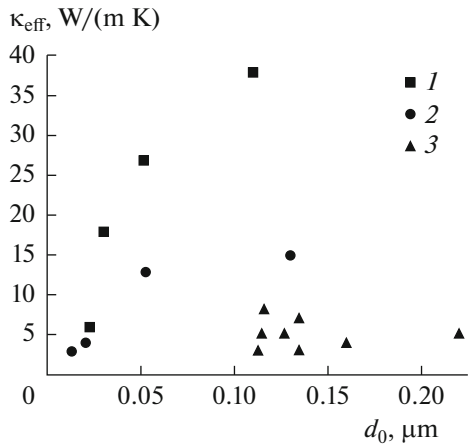

Fig. 2. Dependences of κ_{eff} for different nanowires on their diameters d_0: (*1*) Si nanowires, (*2*) Ge nanowires, and (*3*) Si–Ge nanowire with heterogeneous interface [87].

with an external diameter of 0.073–0.128 μm. The presence of the Si–Ge interface leads to phonon scattering at not only nanowire boundaries but also this interface. For example, it was established in [86] that κ_{eff} for heterogeneous Si–Ge wires is smaller by a factor of 3–4 than that for separate homogeneous Si and Ge wires at their identical diameters (see Fig. 2).

Nanotubes are unique objects because of their structure. They are cylindrical objects with diameter d_0 and length l_0 consisting of a rolled monolayer of material (for example, graphene, boron nitride, etc.). This structure, in turn, provides almost complete absence of boundary phonon scattering and high thermal and electrical conductivities [72]. Depending on the number of monolayers that enter a nanotube, it is customary to separate single-layer and multilayer tubes. It should be noted that the κ_{eff} value for multilayer tubes is smaller [89] than that for single-layer ones, because of phonon scattering at the boundaries of monolayers.

To date, the most investigated objects are carbon nanotubes, some experimental results for which were given in [90–95]. In these studies, thermal properties of single-layer carbon nanotubes with external diameter $d_0 \approx 0.001$–0.03 μm and length $l_0 \approx 1$–10 μm were analyzed. The investigations were performed using techniques based on the application of various thermal nanosensors [90, 91], differential thermometry [92], analysis of I–V characteristics [93], and some other described methods [94].

It is shown in Table 3 that extrema of $\kappa_{eff}(T)$ for carbon nanotubes are observed at close-to-room temperatures ($T_m \approx 280$–320 K); these extrema are $\kappa_{eff}^{max} = 2.40$–$4.74$ kW/(m K) on average and, in some cases [95], may reach even $\kappa_{eff}^{(max)} \approx 9.8$ kW/(m K). Thus, thermal conductivity of carbon nanotubes is much higher than that for bulk samples of different carbon modifications. For example, the $\kappa_{eff\|}^{(max)}$ values of the former exceed by a factor of 5–10 the diamond thermal conductivity (which is $\kappa_\infty \approx 0.9$–$2.3$ kW/(m K) at room temperature) [96].

Analysis of the influence of the sizes of tubes on their thermal properties showed [96] that l_{eff} decreases with an increase in d_0 due to the increase in the number of states (e.g., tube structural defects), from which phonons are scattered. This circumstance, in turn, leads to a decrease in κ_{eff}. For example, $l_{eff} \approx 2.76$ μm and $\kappa_{eff} \approx 8$ kW/(m K) at $d_0 \approx 10^{-3}$ μm and room temperature, whereas for $d_0 \approx 3 \times 10^{-3}$ μm, $l_{eff} \approx 0.75$ μm and $\kappa_{eff} \approx 2$ kW/(m K).

Another parameter that affects κ_{eff} of tubes is their chirality [97]. Due to the structural features of tubes of different chiralities, the amount of heat (and, accordingly, κ_{eff}) transferred by the longitudinal and tangent phonon modes for zigzag configuration [97] is larger [3] as compared with other configurations.

Empirical formulas for estimating κ_{eff} at known T and L values were obtained in [93] based on analysis of the experimental data. Tube length l_0 was chosen as L.

To conclude, we should note that the main difference between heat transfers in the cases of small-size systems and low-temperature macroscopic bodies is that the phenomenon of nondiffusive energy transfer for objects with significantly small sizes ($L \le 10$ μm) can be observed at much higher temperatures (up to room temperature). Another specific feature of heat transfer in small-size structures is significant anisotropy of thermal conductivity κ_{eff}. The theory [13] indicates that this circumstance may lead to different energy-transfer mechanisms for the same object in different directions. For example, it was stated for thin

Table 3. Results of experimental studies on heat transfer in single-layer carbon nanotubes

References	Measurement technique	d_0, 10^{-3} μm	l_0, μm	T_m, K	$k_{eff\|}^{max}$, kW/(m K)	$l_{eff}(T \approx 300\,\text{K})$, μm
[93]	Measurement and analysis of I–V characteristics	1.7	2.6	280–320	2.5–3.3	–
[91]	Stationary thermo- and calorimetry	16	1.89	300–310	1.6–1.7	–
[95]		1–3	3–5	280–320	3–9.8	0.25–0.75

films that the longitudinal and transverse thermal conductivities are mainly related to the hydrodynamic and ballistic mechanisms, respectively. Nevertheless, the presented analysis showed that there is no comprehensive experimental study of these mechanisms and their efficiencies have not been compared.

Though the investigations are currently quite intense, there is no complete information about the specific features of all physical processes implemented upon ballistic and hydrodynamic heat transfers and about a transition from the latter regimes to the diffusive regime. All these problems require further analyses.

CONCLUSIONS

The purpose of this study was to describe the modern state of experimental and theoretical investigations in the extremely promising field that has been intensively developed in recent years: nano thermal physics, which is, in essence, a new line or research in thermal physics. Of course, only a small part of this field is presented here, which, nevertheless, shows that physics and methods of describing heat transport in nanostructures differs significantly from the classical theory of heat conduction. First, they are much more diverse. Second, they are based on the statistical theory, solid-state physics, and quantum mechanics.

The considered type of heat transport is often referred to as diffusive–ballistic because it covers the range of variation in parameter $\mathrm{Kn} = l_\infty/L$ from diffusive ($\mathrm{Kn} \ll 1$) to ballistic ($\mathrm{Kn} \gg 1$). The unusualness of the heat-transport mechanisms in nanostructures is enhanced by the dependence of the effective thermal conductivity on the shape and sizes of objects of study, surface roughness, and heat-flow propagation direction with respect to the geometry of samples. Due to this, practical calculations aimed at determining thermal regimes of real devices (e.g., nanoelectronic circuits) become much more complicated, as compared with modern devices because of a large number of parameters, on which the effective thermal conductivity depends.

A very large amount of information on this problem has accumulated for about 25 years. Therefore, many themes are beyond the scope of this study: heat transport in two-dimensional systems (graphene, graphene ribbons, silicene, etc.), composite materials, Kapitza resistances, and some others. However, even more problems are to be solved. In particular, experimental and theoretical investigation of interaction between phonon gas and walls; problems related to internal heat release under electric current and external electromagnetic field, which have not been considered at all. The problems of heating under electric current induce problems of the kinetics of electron and hole gases in semiconductors. Further progress in nanotechnologies will state new problems (in particular, problems related to analyzing fairly complex systems, including materials of different nature, rather than individual elements).

A separate problem is the training of experts in this field. The point is that they should master not only the fundamentals of thermophysics but also the basic physical principles of heat transfer processes.

REFERENCES

1. Dmitriev, A.S., *Teplovye protsessy v nanostrukturakh* (Thermal Processes in Nanostructures), Moscow: Mosk. Energ. Inst., 2012.
2. Fisher, T.S., *Thermal Energy at the Nanoscale*, Singapore: World Scientific, 2013.
3. Cahill, D.G., Ford, W.K., Goodson, K.E., Mahan, G.D., Madjumar, A., Maris, H.J., Merlin, R., and Phillipot, S.R., *J. Appl. Phys.*, 2003, vol. 93, no. 2, p. 793.
4. Cahill, D.G., Braun, P.V., Chen, G., Clarke, D.R., Fan, S., Goodson, K.E., Keblinski, P., King, W.P., Mahan, G.D., Madjumdar, A., Maris, H.J., Phillipot, S.R., Pop, E., and Shi, L., *Appl. Phys. Rev.*, 2014, vol. 1, no. 1, 011305.
5. Dmitriev, A.S., *Vvedenie v nanoteplofiziku* (Introduction to Nanotermophysics), Moscow: BINOM, 2015.
6. Eletskii, A.V., Zitserman, V.Yu., and Kobzev, G.A., *High Temp.*, 2015, vol. 53, no. 1, p. 130.
7. Eletskii, A.V., Erkimbaev, A.O., Zitserman, V.Yu., Kobzev, G.A., and Trakhtengerts, M.S., *High Temp.*, 2012, vol. 50, no. 4, p. 488.
8. Zhang, Z.M., *Nano/Microscale Heat Transfer*, New York: McGraw-Hill, 2007.
9. Alvarez, F.X. and Jou, D., *J. Appl. Phys.*, 2008, vol. 103, 094321.
10. Peierls, R.E., *Ann. Phys. (New York)*, 1929, vol. 395, p. 1055.
11. Klemens, P., *Solid State Phys.*, 1958, vol. 7, p. 1.
12. Zhu, Y.F., Lian, J.S., and Jiang, Q., *Appl. Phys. Lett.*, 2008, vol. 92, 113101.
13. Dong, Y., Cao, B.-Y., and Guo, Z.-Y., *Phys. E* (Amsterdam, Neth.), 2015, vol. 66, p. 1.
14. Li, D., Xu, Y., Chen, X., Li, B., and Duan, W., *Appl. Phys. Lett.*, 2014, vol. 104, 143108.
15. Tarasov, V.V., *Dokl. Akad. Nauk SSSR*, 1945, vol. 46, no. 1, p. 22.
16. Kittel, C., *Introduction to Solid State Physics*, New York: Wiley, 1953.
17. Sussmann, J.A. and Tellung, A., *Proc. Phys. Soc.*, 1963, vol. 81, p. 1122.
18. Gurzhi, R.N., *Zh. Eksp. Teor. Fiz.*, 1964, vol. 46, no. 2, p. 719.
19. Gurzhi, R.N., *Phys.—Usp.*, 1968, vol. 11, no. 2, p. 255.
20. Red'ko, N.A. and Kogan, V.D., *Zh. Eksp. Teor. Fiz.*, 1991, vol. 33, no. 8, p. 2413.
21. Guyer, R.A. and Krumhansl, J.A., *Phys. Rev.*, 1966, vol. 148, no. 2, p. 766.
22. Guyer, R.A. and Krumhansl, J.A., *Phys. Rev.*, 1966, vol. 148, no. 2, p. 778.
23. Ma, Y., *Appl. Phys. Lett.*, 2012, vol. 101, no. 21, 211905.

24. Lifshits, E.M. and Pitaevskii, L.P., *Fizicheskaya kinetika* (Physical Kinetics), vol. 10 of *Teoreticheskaya Fizika* (Theoretical Physics), Moscow: Nauka, 1979.
25. Guo, Z.-Y., *J. Eng. Thermophys.*, 2006, vol. 27, p. 631.
26. Zou, J. and Balandin, A., *J. Appl. Phys.*, 2001, vol. 89, p. 2932.
27. Walkauskas, S.G., Broido, D.A., Kempa, K., and Reinecke, T.L., *J. Appl. Phys.*, 1999, vol. 85, no. 5, p. 2579.
28. Lu, X., Shen, Z., and Chu, J.H., *J. Appl. Phys.*, 2002, vol. 91, p. 1542.
29. Maldovan, M., *J. Appl. Phys.*, 2011, vol. 110, 034308.
30. Chen, G., *Phys. Rev. Lett.*, 2001, vol. 86, p. 2297.
31. Tang, J.H., Zhao, Y., Zhai, G.X., and Bi, C., *J. Appl. Phys.*, 2011, vol. 110, p. 046102.
32. Wang, M. and Guo, Z.-Y., *Phys. Lett. A*, 2010, vol. 374, p. 4312.
33. Alvarez, F.X., *J. Appl. Phys.*, 2008, vol. 103, 094321.
34. Dong, Y., Cao, B.-Y., and Guo, Z.-Y., *Phys. E* (Amsterdam, Neth.), 2015, vol. 66, p. 1.
35. Alvarez, F.X. and Jou, D., *Appl. Phys. Lett.*, 2007, vol. 90, 083109.
36. Mingo, N. and Broido, D.A., *Nano Lett.*, 2005, vol. 5, no. 7, p. 1221.
37. Landau, L.D. and Lifshits, E.M., *Teoriya uprugosti* (Theory of Elasticity), vol. 7 of *Teoreticheskaya Fizika* (Theoretical Physics), Moscow: Nauka, 1987.
38. Alvarez, F.X., Jou, D., and Sellito, A., *J. Appl. Phys.*, 2009, vol. 105, 014317.
39. Guo, Y. and Wang, M., *Phys. Rep.*, 2015, vol. 595, p. 1.
40. Griffin, Jr.A.J., Brotzen, F.R., and Loos, P.J., *J. Appl. Phys.*, 1994, vol. 75, p. 3761.
41. Silin, V.P., *Vvedenie v kineticheskuyu teoriyu gazov* (Introduction to the Kinetic Theory of Gases), Moscow: Fiz. Inst. im Lebedeva, Ross. Akad. Nauk, 1998.
42. Sellito, A., Alvarez, F.X., and Jou, D., *J. Appl. Phys.*, 2010, vol. 107, 064302.
43. Sellito, A., Alvarez, F.X., and Jou, D., *J. Appl. Phys.*, 2010, vol. 107, 114312.
44. Landau, L.D. and Lifshits, E.M., *Gidrodinamika* (Hydrodynamics), vol. 6 of *Teoreticheskaya Fizika* (Theoretical Physics), Moscow: Nauka, 1986.
45. Wang, M., Yang, N., and Guo, Z.-Y., *J. Appl. Phys.*, 2011, vol. 110, 064310.
46. Devienne, F.M., *Frottement et échanges thermiques dans les gaz rarefies* (Friction and Heat Exchange in Rare Gases), Paris: Gauthier-Villars, 1958.
47. Maldovan, M., *Appl. Phys. Lett.*, 2012, vol. 101, 113110.
48. Soffer, S.B.J., *J. Appl. Phys.*, 1967, vol. 38, p. 1710.
49. Teller, C.R. and Tosser, A.J., *Size Effects in Thin Films*, New York: Elsevier, 1983.
50. Cao, B.-Y. and Guo, Z.-Y., *J. Appl. Phys.*, 2007, vol. 102, 053503.
51. Petters, M.T. and Shi, L., *Adv. Funct. Mater.*, 2009, vol. 19, p. 3918.
52. McGaughey, A.J.H., Landry, E.S., Sellan, D.P., and Amon, C.H., *Appl. Phys. Lett.*, 2011, vol. 99, no. 13, 131904.
53. De Tomas, C., Cantarero, A., Lopeandia, A.F., and Alvarez, F.X., *J. Appl. Phys.*, 2014, vol. 115, no. 16, 164314.
54. Singh, D., Murthy, J.Y., and Fisher, T., *J. Appl. Phys.*, 2011, vol. 110, no. 9, 094312.
55. Zhang, G. and Li, B., *J. Chem. Phys.*, 2005, vol. 123, p. 114714.
56. Wang, J.-S., Wang, J., and Zeng, N., *Phys. Rev. B: Condens. Matter Mater. Phys.*, 2006, vol. 74, 033408.
57. Wang, J.-S., Zeng, N., Wang, J., and Gan, C.K., *Phys. Rev. B: Condens. Matter Mater. Phys.,* 2007, vol. 75, 061128.
58. Lacroix, D., Joulain, K., Terris, D., and Lemonnier, D., *Appl. Phys. Lett.*, 2006, vol. 89, no. 10, 103104.
59. Moore, A.I., Saha, S.K., Prasher, R.S., and Shi, L., *Appl. Phys. Lett.*, 2008, vol. 93, no. 8, 083112.
60. Maruyama, S., *Phys. A* (Amsterdam, Neth.), vol. 323, p. 193.
61. Osman, M.A. and Srivastava, D., *Nanotecnology*, 2001, vol. 12, p. 21.
62. Maldovan, M., *J. Appl. Phys.*, 2012, vol. 111, 024311.
63. Mingo, N. and Broido, D.A., *Phys. Rev. Lett.*, 2004, vol. 93, 246106.
64. Casimir, H.B.G., *Phys. A* (Amsterdam, Neth.), 1938, vol. 5, p. 495.
65. Mezhov-Deglin, L.P., *Zh. Eksp. Teor. Fiz.*, 1965, vol. 49, no. 3, p. 66.
66. Mezhov-Deglin, L.P., *Zh. Eksp. Teor. Fiz.*, 1964, vol. 46, no. 5, p. 1926.
67. Zholonko, N.N., *Phys. Solid State*, 2006, vol. 48, no. 9, p. 1678.
68. Zholonko, N.N., Gorodilov, B.Ya., and Krivchikov, A.I., *Pis'ma Zh. Eksp. Teor. Fiz.*, 1992, vol. 55, no. 3, p. 174.
69. Zhernov, A.P., *Fiz. Tverd. Tela (S.-Peterburg)*, 1992, vol. 41, no. 7, p. 1158.
70. Zhernov, A.P. and Zhernov, D.A., *Phys. Solid State*, 1998, vol. 40, no. 9, p. 1456.
71. Ziman, J.M., *Electrons and Phonons: The Theory of Transport Phenomena in Solids*, Oxford: Oxford University Press, 1962.
72. *Springer Handbook of Nanotechnology*, Bhushan, B., Ed., Springer, 2010, vol. 1.
73. Aubain, M.S. and Bandaru, P.R., *J. Appl. Phys.*, 2011, vol. 110, 084313.
74. Johnson, J.A., Maznev, A.A., Cuffe, J., Eliason, J.K., Minnich, A.J., Kehoe, T., Sotomayor, TorresC.M., Chen, G., and Nelson, K.A., *Phys. Rev. Lett.*, 2013, vol. 110, no. 2, 025901.
75. *Tablitsy fizicheskikh velichin. Spravochnik* (Tables of Physical Quantities: Handbook), Kikoin, I.K., Ed., Moscow: Atomizdat, 1976.
76. Celler, G.K. and Cristoloveanu, S., *J. Appl. Phys.*, 2003, vol. 93, no. 9, p. 4955.
77. Sungtaek, JuY., *Appl. Phys. Lett.*, 2005, vol. 87, no. 15, 153106.
78. Liu, W. and Asheghi, M., *Appl. Phys. Lett.*, 2004, vol. 84, no. 19, p. 3819.
79. Asheghi, M., Leung, Y.K., Wong, S.S., and Goodson, K.E., *Appl. Phys. Lett.*, 1997, vol. 71, no. 13, p. 1798.

80. Asheghi, M., Kurabayashi, K., Kasnavi, R., and Goodson, K.E., *J. Appl. Phys.*, 2002, vol. 91, no. 8, p. 5079.
81. Ju, Y.S. and Goodson, K.E., *Appl. Phys. Lett.*, 1999, vol. 74, no. 20, p. 3005.
82. Asheghi, M., Touzelbaev, M.N., Goodson, K.E., Leung, Y.K., and Wong, S.S., *J. Heat Transfer*, 1998, vol. 120, no. 1, p. 30.
83. Blakemore, J.S., *Solid State Physics*, Cambridge: Cambridge Univ. Press, 1987.
84. Siemens, M.E., Li, Q., Yang, R., Nelson, K.A., Anderson, E.H., Murnane, M.M., and Kapteyn, H.C., *Nat. Mater.*, 2009, vol. 9, no. 1, p. 26.
85. Li, D., Wu, Y., Kim, Ph., Shi, L., Yang, P., and Majumdar, A., *Appl. Phys. Lett.*, 2003, vol. 83, no. 14, p. 2934.
86. Hsiao, T.K., Huang, B.W., Chang, H.K., Liou, S.C., Chu, M.W., Lee, S.C., and Chang, C.W., *Phys. Rev. B: Condens. Matter Mater. Phys.,* 2015, vol. 91, p. 035406.
87. Hsiao, T.K., Chang, H.K., Liou, S.C., Chu, M.W., Lee, S.C., and Chang, C.W., *Nat. Nanotechnol.*, 2013, vol. 8, p. 534.
88. Dmitriev, A.S. and Timokhov, N.V., *Vestn. Mosk. Energ. Inst.*, 2006, no. 6, p. 125.
89. Park, J.G., Cheng, Q., Lu, J., Bao, J., Tian, Y., Liang, R., Wang, B., Zhang, Ch., and Brooks, J.S., in *Proc. 18th Int. Conf. on Composite Materials 2011.* http://www.iccmentral.org/Proceedings/ICCM18proceedings/data/2.%20Oral%20Presentation/Aug23(Tuesday)/T36%20Nanocomposites/T36-3-AF0345.pdf.
90. Hone, J., Llaguno, M.C., Nemes, N.M., Johnson, A.T., Fischer, J.E., Walters, D.A., Casavant, M.J., Schmidt, J., and Smalley, R.E., *Appl. Phys. Lett.*, 2000, vol. 77, no. 5, p. 666.
91. Fujii, M., Zhang, X., Xie, H., Ago, H., Takahashi, K., Ikuta, T., Abe, H., and Shimizu, T., *Phys. Rev. Lett.*, 2005, vol. 95, no. 6, 065502.
92. Hone, J., Whitney, M., Piskoti, C., and Zettl, A., *Phys. Rev. B: Condens. Matter Mater. Phys.,* 1999, vol. 59, no. 4, p. 2514.
93. Pop, E., Mann, D., Wang, Q., Goodson, K.E., and Dai, H., *Nano Lett.*, 2006, vol. 6, no. 1, p. 96.
94. Cahill, D.G., Goodson, K.E., and Majumdar, A., *J. Heat Transfer*, 2002, vol. 124, no. 2, p. 223.
95. Yu, Ch., Shi, L., Yao, Sh., Li, D., and Majumda, A., *Nano Lett.*, 2005, vol. 5, no. 9, p. 1842.
96. Wei, L., Kuo, P.K., Thomas, R.L., Anthony, T.R., and Banholzer, W.F., *Phys. Rev. Lett.*, 1993, vol. 70, no. 24, p. 3764.
97. Eletskii, A.V., *Phys.—Usp.*, 2002, vol. 45, no. 1, p. 369.

Translated by A. Sin'kov